NASA TECHNICAL NOTE

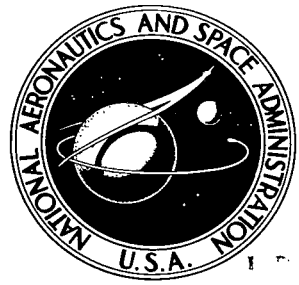

NASA TN D-8388

OXIDATION IN OXYGEN AT 900° AND 1000° C OF FOUR NICKEL-BASE CAST SUPERALLOYS: NASA-TRW VIA, B-1900, ALLOY 713C, AND IN-738

George C. Fryburg, Fred J. Kohl, and Carl A. Stearns

Lewis Research Center
Cleveland, Ohio 44135

NATIONAL AERONAUTICS AND SPACE ADMINISTRATION • WASHINGTON, D. C. • JANUARY 1977

1. Report No. NASA TN D-8388	2. Government Accession No.	3. Recipient's Catalog No.
4. Title and Subtitle OXIDATION IN OXYGEN AT 900° AND 1000° C OF FOUR NICKEL-BASE CAST SUPERALLOYS: NASA-TRW VIA, B-1900, ALLOY 713C, AND IN-738.		5. Report Date January 1977 6. Performing Organization Code
7. Author(s) George C. Fryburg, Fred J. Kohl, and Carl A. Stearns		8. Performing Organization Report No. E-8770
9. Performing Organization Name and Address Lewis Research Center National Aeronautics and Space Administration Cleveland, Ohio 44135		10. Work Unit No. 506-16 11. Contract or Grant No.
12. Sponsoring Agency Name and Address National Aeronautics and Space Administration Washington, D.C. 20546		13. Type of Report and Period Covered Technical Note 14. Sponsoring Agency Code

15. Supplementary Notes

16. Abstract

The oxidation at 900° and 1000° C of four nickel-base superalloys in 1 atmosphere of slowly flowing oxygen has been investigated. Thermogravimetric rate data were obtained for periods to 100 hours. The morphology and composition of the oxide scales formed after 100 hours were studied by optical microscopy, X-ray diffraction, electron microprobe, scanning electron microscopy, and X-ray photoelectron spectroscopy (ESCA). Alloys B-1900 and VIA were found to be primarily alumina formers, though probably 25 percent of their surface was covered by Cr_2O_3-containing oxides at 900° C. Alloys 713C and IN-738 were primarily chromia formers, though the surface of 713C at 1000° C was covered with NiO and the surface of IN-738 at both temperatures was covered with a thin layer of TiO_2.

17. Key Words (Suggested by Author(s)) Oxidation; Heat-resistant alloys; Chromium oxides; Aluminum oxides; Titanium oxides; Thermogravimetry

18. Distribution Statement Unclassified - unlimited
STAR Category 26

19. Security Classif. (of this report)	20. Security Classif. (of this page)	21. No. of Pages	22. Price*
Unclassified	Unclassified	44	$4.00

* For sale by the National Technical Information Service, Springfield, Virginia 22161

OXIDATION IN OXYGEN AT 900° AND 1000° C OF FOUR NICKEL-BASE CAST SUPERALLOYS: NASA-TRW VIA, B-1900, ALLOY 713C, AND IN-738

by George C. Fryburg, Fred J. Kohl, and Carl A. Stearns

Lewis Research Center

SUMMARY

The oxidation at 900° and 1000° C of four nickel-base superalloys in 1 atmosphere of slowly flowing oxygen has been investigated. Thermogravimetric rate data were obtained for periods to 100 hours. The morphology and composition of the oxide scales formed after 100 hours were studied by optical microscopy, X-ray diffraction, electron microprobe, scanning electron microscopy, and X-ray photoelectron spectroscopy (electron spectroscopy for chemical analysis (ESCA)). Alloys B-1900 and VIA were found to be primarily alumina formers, though probably 25 percent of their surface was covered by Cr_2O_3-containing oxides at 900° C. Alloys 713C and IN-738 were primarily chromia formers, though the surface of 713C at 1000° C was covered with NiO and the surface of IN-738 at both temperatures was covered with a thin layer of TiO_2.

INTRODUCTION

As part of a larger program aimed at understanding the chemical mechanism of "hot corrosion," we have investigated the oxidation of four nickel-base, cast superalloys in 1 atmosphere of slowly flowing oxygen. As a basis of comparison for the hot-corrosion studies, thermogravimetric determinations of the rate of oxidation were made at 900° and 1000° C. In addition, extensive studies were made to define the morphology and composition of the oxide scales formed on these alloys after 100 hours of oxidation in oxygen. This is of interest because it is anticipated that hot-corrosion studies will be performed on specimens preoxidized in this manner, and the morphology and composition of the oxide scales will certainly be a determining factor in the mechanism of initiation of hot corrosion. Since it is known (refs. 1 and 2) that oxide structures are temperature, pressure, and time dependent, we felt it necessary to examine the scales formed after 100 hours of oxidation under the conditions of our hot-corrosion experiments.

Commercial superalloys of the type examined in this study are generally divided into two groups depending on the composition, morphology, and growth kinetics of the oxide scale (refs. 1 and 2). One group is designated as "alumina formers;" the other group, as "chromia formers." The alumina formers are characterized by a nonparabolic, nearly logarithmic rate law with weight gains of the order of 0.2 to 0.5 milligram per square centimeter at temperatures of 900° and 1000° C. The scale morphology is characterized by a thin, continuous layer of Al_2O_3 adjacent to the metal substrate. The Al_2O_3 layer may be covered by an external layer of another oxide, or other oxides may be dissolved in it. The nature of these oxides depends on the alloy composition. Generally, internal oxidation beneath the continuous scale is absent. The "chromia formers" are characterized by a parabolic, or paralinear, rate law with weight gains of the order of 1 to 5 milligrams per square centimeter after 100 hours at 900° or 1000° C. The scale morphology is characterized by a predominant Cr_2O_3 layer with internal oxidation of aluminum just beneath, resulting in "tentacles" of Al_2O_3 directed into the alloy. Other oxides may be dissolved in the Cr_2O_3 layer, and layers of other oxides may exist above or below the Cr_2O_3 layer. Again the nature of the oxides depends on the composition of the alloy.

While it is an oversimplification to classify superalloys as either alumina formers or chromia formers, the distinction is convenient and the practice will be used in this report. However, it must be kept in mind that the oxide scales are, in reality, a complicated mixture of several individual oxides the nature of which depends on many factors.

The oxide scales were examined by conventional techniques: X-ray diffraction, electron microprobe, scanning electron microscope, and optical microscopy. In addition, the scales were examined by the technique of X-ray photoelectron spectroscopy (electron spectroscopy for chemical analysis (ESCA)) to ascertain the applicability of this method to such oxidation studies and the possibility of extending it to hot-corrosion studies.

EXPERIMENTAL TECHNIQUES

The alloy samples were obtained from commercial sources and had been given the following conventional heat treatments in argon:

(1) NASA-TRW VIA: 32 hours at 900° C, air cooled

(2) B-1900: 4 hours at 1080° C, air cooled

(3) Alloy 713C: no treatment

(4) IN-738: 2 hours at 1120° C, air cooled

The chemical analyses and the microstructures of the samples have been reported by Barrett, et al. (ref. 3) and are typical of the alloys. The analyses are given here in

table I, in which the compositions are expressed as atomic percent as well as weight percent.

The samples were cut to a size in centimeters of 0.2 by 1.0 by 2.5. A hanger-hole was drilled in one end and all surfaces were glass-bead blasted to give a uniform matte surface. The samples were cleaned ultrasonically in chloroform and in detergent; then rinsed with water, acetone, and ethanol.

Isothermal oxidations were carried out at 900° and 1000° C in slowly flowing oxygen at atmospheric pressure. The direction of flow was downward and the speed was approximately 20 centimeters per minute. Continuous gravimetric measurements were made with a Cahn R-100 electrobalance having a 100-gram capacity and a sensitivity of 1 microgram. Samples were suspended by platinum/13-percent-rhodium chains into the hot zone of a tube furnace. The temperature of the furance was regulated to ±2 degrees C with a precision set-point, proportional silicon-controlled-rectifier (SCR) controller.

The furnace was mounted on a vertical track and was counterweighted to facilitate raising and lowering around the sample. A quartz furnace tube, 2.5 centimeters in outside diameter, was used to enclose the specimen. The temperature of the specimen was measured with a platinum/platinum-13-percent-rhodium thermocouple sheathed with a 0.4-centimeter-outside-diameter, thin-wall quartz tube and positioned just below the hanging specimen. Corrections were made for the difference in temperature between the specimen and the thermocouple. The corrections were determined from blank specimens that were thermocoupled.

Experiments were begun by raising the heated furnace around the hanging specimen; the oxygen flow had been adjusted at least 1 hour previously. Corrections in the weight change were made for the buoyancy effect. Exposure times were approximately 100 hours.

X-ray diffraction analyses were made of the oxide scales on the samples. Subsequently, the samples were coated with a thin layer of copper in an evaporator and then with a thicker layer by electroplating. They were mounted in epoxy and sectioned along their long axis. After polishing they were etched with an oxidizing etchant: 33 water, 33 nitric acid, 33 acetic acid, and 1 hydrofluoric acid.

The mounted samples were examined by optical microscopy and electron microprobe techniques. For the latter, the specimens were vacuum-evaporation coated with a few hundredths of a micrometer of carbon or gold, and microprobe backscatter electron micrographs and elemental X-ray micrographs were obtained on selected areas for several elements of concern. The samples were also examined in the scanning electron microscope (SEM) at higher magnification. X-ray energy dispersive spectra (EDS) were obtained for various positions in the oxide scales to determine the elements present.

Extensive studies were undertaken to examine the oxide scales by the ESCA tech-

nique to determine if useful information could be obtained[1] (ref. 4). Separate specially prepared samples were examined with a Varian IEE-15 X-ray photoelectron spectrometer equipped with a high-intensity magnesium anode (K_α radiation, 1253.6 eV). The samples were cylindrical, with a diameter of 1.1 centimeters and a height of 1.9 centimeters. They were oxidized in the thermogravimetric apparatus and stored in a desicator until insertion into the ESCA instrument. The cylindrical surface was the area exposed to the exciting X-rays.

RESULTS AND DISCUSSION

Thermogravimetric Rate Studies

Samples of the four alloys were subjected to oxidation in 1 atmosphere of slowly flowing oxygen at 900° and 1000° C for 100-hour periods. Typical weight gains recorded are presented in figures 1 and 2. Check runs made on the individual alloys generally were reproducible to better than ±25 percent.

As expected (ref. 3), B-1900 was the most resistant to oxidation, followed closely by VIA. There was little increase in rate at the higher temperature, especially with B-1900, which seemed to be simultaneously losing weight from oxidation of Cr_2O_3 to the volatile CrO_3 (ref. 5). Alloy 713C oxidized to a greater extent than B-1900 and VIA and was more like 738, especially at 900° C.

The results at 1000° C may be compared with the results of Barrett, et al. (ref. 3) for these four alloys oxidized in static air. The weight gains for VIA and B-1900 are the same in oxygen and air within experimental error, though B-1900 tends to be a little lower in flowing oxygen probably because of a greater rate of loss of $CrO_3(g)$ from the surface. The weight gain for 713C in flowing oxygen in seven times greater than in static air; and for 738, it is three times greater. Check runs in static air in our apparatus confirmed these differences. The differences undoubtedly arise from variations in the composition of the oxide scale formed under the two conditions. Apparently, the highly protective layer of Al_2O_3 formed on 713C in air is not being formed as readily in oxygen, and Cr_2O_3 or spinels are forming instead.

As is evident from the rate curves, the data for B-1900 and VIA could not be fitted to a parabolic rate law. However, the data for 713C and 738 were so treated. The data for 713C at 900° C obeyed the parabolic law out to 50 hours. However, the data at 1000° C fell off from parabolic at very short times and no rate constant could be ob-

[1]Electron spectra of our oxidized samples were obtained by G. D. Mateescu and W. J. Carter III at Case Western Reserve University under NASA Grant NSG-3009. For more detail on the procedure and the method of analysis, see ref. 4.

tained. The data for 738 at 900° C obeyed the parabolic law out to 100 hours; and the data at 1000° C, out to 50 hours. The parabolic rate constants obtained from the data by linear regression analysis are presented in table II. On the basis of the growth rate studies, we would classify B-1900 and VIA as alumina formers and 713C and 738 as chromia formers, under the conditions of our experiments.

Oxide Scale Studies

Several techniques were used to try to determine the morphology and composition of the oxide scales formed. The results of each method are discussed in turn, and in a final section all the results are correlated.

Optical microscopy. - Light micrographs of cross sections of typical regions of the oxide scale are shown in figures 3 to 6 for the four alloys oxidized at 900° and 1000° C for 100 hours. All specimens exhibited γ' depletion zones below the scale. In addition, many specimens exhibited a region of internal oxidation (ref. 6) below the surface scale. The thicknesses of all these regions were measured and the results are given in table III.

The oxide scale formed on B-1900 at 900° C (fig. 3(a)) consisted primarily of a thin layer (gray in the photograph) that appeared to be continuous and adherent. However, an appreciable fraction of the surface, roughly 25 percent, exhibited regions in which the oxide scale was thicker and displayed internal oxidation beneath the scale (left side of fig. 3(a)). At 1000° C (fig. 3(b)) the continuous scale was a little thicker and no regions exhibiting internal oxidation were evident.

The morphology of the oxide on VIA (figs. 4(a) and (b)) was about the same as of that on B-1900: the thicknesses of the scale and the depletion zones were comparable at 900° C and slightly greater at 1000° C.

The oxide on 713C at 900° C (fig. 5(a)) was different from that on B-1900 and VIA in that the entire sample exhibited internal oxidation beneath the continuous outer scale. Both the scale and the oxide tentacles were thicker than on B-1900 and VIA. The oxide formed at 1000° C (fig. 5(b)) was thicker than that formed at 900° C, and the tentacles had merged into a nearly continuous sublayer. Some spalling of this oxide frequently occurred upon cooling to room temperature, but the portion depicted here is an unspalled portion.

The oxide formed on 738 at 900° C (fig. 6(a)) also displayed a zone of internal oxidation beneath the continuous outer scale. The continuous scale consisted of two layers: a thin, light outer layer (gray in the photograph) and a much thicker inner layer. At 1000° C (fig. 6(b)) the oxidation was even more extensive; the morphology was similar to the scale formed at 900° C, with internal oxidation resulting in long oxide tentacles extending into the alloy. Some spalling of this oxide frequently occurred upon cooling,

but the area shown here is of an unspalled portion.

X-ray diffraction analysis. - Identification of oxide phases was often difficult, especially on B-1900 and VIA, partly because of the thinness of the oxide layer and partly because of the similarity in the patterns of many of the possible compounds. This was particularly true of a pattern identified as tapiolite (ref. 7) that has the general formula $(Ni, Co)(Ta, Nb)_2O_6$. The cations in tapiolite can vary over wide limits, resulting in variations in the "d values" of the pattern. In addition, the ASTM cards for $Cr(Ta, Nb)_2O_6$ and $Cr(Ta, Nb)O_4$ are very similar to that for tapiolite. The phase, which is called tapiolite in this report, is probably $(Ni, Co, Cr)(Ta, Nb, W, Mo)_2O_6$.

The spinels formed on the various alloys ranged in lattice parameter from that corresponding to $NiAl_2O_4$ ($a_o = 8.05 \times 10^{-10}$ m) to $NiCr_2O_4$ ($a_o = 8.3 \times 10^{-10}$ m). In some cases, both these spinels formed as indicated by distinct diffraction peaks for the two phases; in other cases the peaks were smeared out or merged into single peaks with a lattice parameter intermediate between $NiAl_2O_4$ and $NiCr_2O_4$, indicating a mixed spinel.

It was also difficult to detect NiO in the oxide scales unless it was present as a major constituent. This resulted from the fact that the strong NiO lines are concurrent with strong lines of either Al_2O_3 and Cr_2O_3 or their spinels.

The oxide phases identified on the samples that had been oxidized for 100 hours are presented in table IV. The phases are listed in order of decreasing intensity of their diffraction patterns, though this is not necessarily related to their relative quantity on the sample. In all cases the nickel alloy solid-solution phase was observed, showing that the X-rays penetrated through the oxide scale.

The X-ray diffraction analysis revealed that the oxide scales on these four alloys were a complex mixture of as many as five different oxides. The patterns for B-1900 and VIA were very similar at both temperatures and indicated the presence of tapiolite, α-Al_2O_3, and spinels. The most notable feature was the increased intensity of α-Al_2O_3 in the scales formed at 1000° C as compared with those formed at 900° C.

The scale formed on 713C at 900° C, being predominately Cr_2O_3, was different from that formed on B-1900 and VIA. At 1000° C some of the 713C specimens tended to spall. A thin, black, surface oxide popped off to reveal a greenish oxide underneath. This occurred over 25 percent of the surface at most. X-ray diffraction revealed that the spalled oxide was primarily NiO with chromium spinel and Cr_2O_3. The retained scale appeared to be chromium spinel with Cr_2O_3, Al_2O_3, and a little tapiolite.

The scale formed on 738 was predominately Cr_2O_3 and TiO_2 at both temperatures. The scales formed at 1000° C also frequently tended to spall upon cooling. Diffraction patterns showed the spall to be TiO_2 and Cr_2O_3. The retained scale was Cr_2O_3 and a little tapiolite.

The X-ray diffraction technique gives an indication of the oxide phases present in the scales. Their position and relative importance are discussed in more detail later in this report.

ESCA analysis. - The ESCA technique is primarily a surface analysis technique (ref. 8); the escape depth of the secondary electrons was no more than roughly 0.005 micrometer, depending on the element in question. The technique identifies the elements in the surface and their oxidation state. In table IV we present the relative abundance of oxidized metals and their oxidation state found by ESCA on the oxide scales formed at 900° and 1000° C on the four alloys (ref. 4).

The most striking feature of these results is the large fraction of oxidized titanium found in the surface of the scales as compared with the small amount present in the alloys: alloys B-1900, VIA, and 713C contained only 1-atomic-percent titanium; and 738, only 4 atomic percent. This feature was especially true for the scales formed at 900° C. The result was not indicated by the X-ray diffraction data (except for 738), probably because the TiO_2 dissolved in one of the other oxides.

Electron microprobe analysis. - The sample areas shown in the optical micrographs of figures 3 to 6 were examined with the electron microprobe. Elemental X-ray micrographs for seven or eight elements, including oxygen, were obtained. These micrographs, along with the back-scattered or secondary electron micrographs of the same areas, are presented in figures 7 to 14 for the four alloys.

For B-1900 at 900° C (fig. 7), aluminum was distributed throughout the oxide, but titanium was essentially concentrated along the surface. Chromium was evident in the surface oxide above the region in which internal oxidation had taken place, and the oxide tentacles in this region were primarily aluminum. Some tantalum was evident at one spot in the oxide. At 1000° C (fig. 8) the oxide seemed to be composed primarily of aluminum. A few areas of greatest attach exhibited concentrations of titanium and tantalum and were probably carbides of these elements in the surface prior to oxidation. Both titanium and tantalum carbides were evident in the alloy.

For VIA at 900° C (fig. 9) the oxide was very similar to that on B-1900 at the same temperature. At 1000° C (fig. 10), where the oxidation was more extensive, both titanium and chromium appeared throughout the upper portion of the oxide, and aluminum was concentrated in a layer along the inner surface of the oxide. Spotty concentrations of nickel, tantalum, and even tungsten appeared in the region of greatest attack. This was probably a surface carbide.

For 713C at 900° C (fig. 11) the continuous outer layer of oxide was composed of titanium and chromium. The tentacles of oxide extending inward from the outer layer appeared to be primarily aluminum. Nickel seemed to be depleted in the oxide. Niobium and molybdenum showed no concentration in the oxide, but niobium was concentrated as a carbide in the alloy. The depletion zone was low in titanium and aluminum. At 1000° C (fig. 12) the continuous, gray outer layer (in the electron micrograph) was composed primarily of chromium and titanium, along with nickel. The underlying portion was primarily aluminum with some molybdenum and again, nickel.

For 738 at 900° C (fig. 13) the thin outer layer of the oxide was composed primarily

of titanium, and the thicker inner layer showed a high concentration of chromium. The tentacles extending into the alloy had a high concentration of aluminum. Titanium was also partly distributed throughout the inner layer and the tentacles. There might have been a slight segregation of tantalum in the oxide, but tungsten exhibited no segregation. Nickel was depleted in the oxide. The depletion layer was low in chromium, aluminum, and titanium. At 1000° C (fig. 14), the morphology of the oxide was very similar to that formed at 900° C, but oxidation had been more extensive. There was a definite segregation of tantalum just beneath the thick inner layer of oxidized chromium and just above the tentacles of internally oxidized aluminum.

Scanning electron microscope studies. - The scanning electron microscope (SEM) was used to examine the samples, primarily because of its high magnification. It was especially useful for B-1900 and VIA, which formed comparatively thin oxide scales. X-ray energy dispersive spectrometry (EDS) was performed on selected areas of the scales, as indicated on the micrographs in figures 15 to 21. The spectrometer was operated in the "spot" mode, usually at a magnification three times that shown in the electron micrographs. The analyses agreed with the results of the elemental X-ray micrographs obtained in the electron microprobe analysis but in some instances yielded additional information because of the greater magnification. It should be noted that, though the SEM micrographs are of the same areas shown in the microprobe and light micrographs, they are mirror images of these.

The SEM micrographs of the oxide scale on B-1900 oxidized at 900° C are presented in figure 15. This is a higher magnification micrograph of the left side of figure 3(a), which displayed the internal oxidation feature. The oxide consisted of a thin, continuous (gray) layer with short (black) tentacles extending into the alloy. Spot EDS spectra of the different morphologies, also presented in figure 15, reveal that the continuous layer (spot 1) was primarily chromium and titanium with some nickel and cobalt and that the (black) tentacles (spot 2) were primarily aluminum. No corrections were made on the detected X-ray intensities; consequently, the relative peak heights cannot be used directly to read the chemical composition. Nevertheless, the EDS spectrum of the alloy of known composition, also shown in figure 15, gives an indication of the relative composition. (This alloy spectrum was obtained from the sample oxidized at 1000° C that was coated with carbon instead of gold.)

The B-1900 sample oxidized at 1000° C exhibited a continuous (gray) layer of oxide (fig. 16). Spot EDS spectra reveal that this oxide was primarily aluminum with some nickel, cobalt, and chromium.

The oxide scales formed on VIA at 900° and 1000° C were similar to those formed on B-1900, with respect to both the morphology and the composition, as indicated by the EDS spectra. The SEM micrographs and the spot EDS spectra are shown in figures 17 and 18.

The SEM micrographs of the oxide scale formed on 713C at 900° C are presented in

figure 19 along with the EDS spectra. The results corroborate the optical and microprobe data; that is, the outer oxide layer (spot 1) was primarily chromium with some titanium and the tentacles (spot 2) were primarily aluminum. The data for 713C at 1000° C (fig. 20) show that the oxide scale was continuous and appeared to be composed of three layers. An outer layer (light gray), revealed in the high-magnification micrograph (spot 1), was mostly nickel with a little chromium. A middle layer (darker gray; spot 2) was mostly chromium with appreciable amounts of nickel and titanium. The innermost layer exhibited black tentacle-like structures (spot 4) composed primarily of aluminum with a little nickel and chromium, encompassing white areas (spot 3) composed of pure nickel.

The SEM micrographs of the oxide scale formed on 738 at 900° C (fig. 21) displayed a thin outer layer (dark gray) on a thick inner layer (light gray) from which dark tentacles extended into the alloy. The EDS spectra showed that the outer layer (spot 1) was composed mostly of titanium with a little chromium and that the thick inner layer (spot 2) was mostly chromium with some titanium. The tentacles (spot 3) were primarily aluminum with a little titanium and chromium. The oxide formed on 738 at 1000° C displayed the same morphology as that formed at 900° C, except that the various components were thicker. The EDS spectra for 738 at 1000° C were nearly identical to those shown in figure 21 and so are not presented.

Summary of Oxide Scale Identification

Results of oxide scale studies are discussed alloy by alloy.

B-1900. - At 900° C the oxide scale on B-1900 consisted primarily of a thin layer of Al_2O_3 with TiO_2 dissolved in it, the TiO_2 being concentrated toward the outer surface. This is typical of the oxide formed on alumina formers. However, other areas exhibited an outer layer of Cr_2O_3 with TiO_2 and NiO; again the TiO_2 was concentrated along the outer surface. Mixed spinels occurred from the NiO, while the TiO_2 appeared to be dissolved in the Cr_2O_3. Beneath the areas with the Cr_2O_3 outer layer, internal oxidation of aluminum occurred, with the formation of tentacles of Al_2O_3. This type of scale is more typical of the chromia formers and demonstrates that different areas on the same alloy may exhibit different types of scales. Areas of tapiolite were formed where surface carbide particles were oxidized, the carbides being tantalum and titanium carbides.

It seems plausible to use the ESCA data for this sample to estimate what proportion of the sample surface was covered with the Al_2O_3 type of scale and what proportion was covered with the Cr_2O_3 type of scale. Roughly, three times as much surface was covered with Al_2O_3 as with Cr_2O_3 (table IV, column 4); that is, 75 percent of the surface was covered with Al_2O_3 and 25 percent with Cr_2O_3. This figure agrees roughly

with the light-micrograph observations of the oxide cross sections described previously. This interpretation of the ESCA data is an oversimplification as it neglects the fact that Cr_2O_3 and Al_2O_3 are mutually soluble. Nevertheless, the hypothesis may be used as a first approximation.

At 1000° C the oxide scale on B-1900 consisted of a continuous layer of Al_2O_3 with some NiO and a little Cr_2O_3 dissolved in it. Little or no TiO_2 was evident except where carbide particles lay in the surface. Here TiO_2 and Ta_2O_5 occurred: the former in solid solution, the latter as tapiolite. The scale is more typical of an alumina former. The ESCA data (table IV, column 4) corroborate the greater prominence of aluminum in the oxide scale at the higher temperature. This was also disclosed by the X-ray diffraction results. In addition, the ESCA data corroborate the decreased prominence of titanium in the oxide at 1000° C.

NASA-TRW VIA. - At 900° C the composition and morphology of the oxide on VIA were nearly identical with those of the oxide on B-1900. Tapiolite was a little more prevalent, reflecting the higher percentage of tantalum in this alloy. At 1000° C the scales were also very similar but with the scale on VIA exhibiting a higher percentage of tapiolite and of chromium and aluminum spinels. The ESCA data for VIA were almost identical to those for B-1900 and thus may be given the same interpretation; that is, at 900° C about 75 percent of the surface of the specimen was covered with the Al_2O_3 type of scale and 25 percent with the Cr_2O_3 type of scale. Likewise, at 1000° C the ESCA data corroborate the greater prominence of aluminum on the surfaces and the decrease in the amount of titanium.

Alloy 713C. - The oxide scale on 713C at 900° C consisted of a continuous, gray layer of Cr_2O_3 with a little TiO_2 in solid solution concentrated along the outer surface. Below this layer, internal oxidation of aluminum resulted in tentacles of Al_2O_3. Little or no areas existed with the thin Al_2O_3 type of layer that formed on this alloy in air. In oxygen the alloy appeared to be predominately a chromia former.

At 1000° C the scale on 713C consisted of a thin outer layer of NiO that had a tendency to spall when the sample was cooled to room temperature. Beneath the NiO layer was a thicker layer composed of a complicated mixture of Cr_2O_3, TiO_2, and NiO that resulted primarily in chromium spinel. The innermost portion was mostly tentacled Al_2O_3 surrounding areas of NiO, the Al_2O_3 forming a nearly continuous layer. Some niobium and molybdenum oxidation was indicated in this lower portion of the scale and resulted in the formation of tapiolite.

IN-738. - At 900° C the oxide on IN-738 consisted of a dual scale: thin outer layer of TiO_2, with some Cr_2O_3 in solid solution, that was almost continuous and appeared to cover a large part of the surface; and a thick, continuous inner layer of Cr_2O_3 with some TiO_2 in solid solution. Extensive internal oxidation occurred beneath this dual layer, resulting in long Al_2O_3 tentacles with some TiO_2 dissolved in them.

At 1000° C the oxide on 738 exhibited the same morphology, but oxidation was more

extensive. There was some oxidized tantalum beneath the Cr_2O_3 layer, giving rise to tapiolite. The scales at both temperatures were typical of chromia formers. The thicker scale formed at 1000° C tended to spall upon cooling to room temperature. The TiO_2 layer tended to flake off and carry a small portion of the Cr_2O_3 layer with it.

Results of the present investigation have revealed the complexity of the oxide scales formed on four typical nickel-base superalloys and have demonstrated what a gross oversimplification it would be, in studying hot-corrosion mechanisms, to consider various alloys as having just an Al_2O_3 oxide scale or just a Cr_2O_3 oxide scale.

CONCLUDING REMARKS

In this study, five different experimental techniques were applied to determining the morphology and composition of the complex oxide scales formed on nickel-base superalloys oxidized at high temperature. The light microscope and X-ray diffraction analyses have been used for many years and were almost the only techniques available for some time. More recently, the electron microprobe, with its elemental X-ray micrographs, and the scanning electron microscope, with its X-ray energy dispersive spectra, have been used to supplement the older techniques. Each technique offers its own unique advantages, and results from all were useful in interpreting these complex oxide scales.

We have also applied the technique of X-ray photoelectron spectroscopy (ESCA) to the examination of oxide scales. ESCA is a macroscopic tool and gives an averaged measurement for an area of several square centimeters. The measurements showed that ESCA can give a sensitive indication of the elements in the surfaces of oxide scales (i. e., in the top 0.005 μm), and the results are amenable to quantitative interpretation. Although the ESCA results were not critical in the analysis of the thick oxide scales formed in this study, the technique, nevertheless, provided useful supplementary information. It would probably be a powerful tool in studying the very early stages of oxidation, although it was not used for that purpose in this study.

Lewis Research Center,
National Aeronautics and Space Administration,
Cleveland, Ohio, September 21, 1976,
506-16.

REFERENCES

1. Wright, I. G.: Oxidation of Iron- Nickel- and Cobalt-Base Alloys. MCIC-72-07, Metals and Ceramic Information Center (AD-745473), 1972.

2. Wasielewski, Gerald E.; and Rapp, Robert A.: High-Temperature Oxidation. The Superalloys. Chester T. Sims, ed., Ch. 10, John Wiley & Sons, Inc., 1972, pp. 287-316.

3. Barrett, Charles A.; Santoro, Gilbert J.; and Lowell, Carl E.: Isothermal and Cyclic Oxidation at 1000° and 1100° C of Four Nickel-Base Alloys: NASA-TRW VIA, B-1900, 713C, and 738X. NASA TN D-7484, 1973.

4. Mateescu, Gheorghe D.: An X-Ray Photoelectron Spectroscopy Study of Nickel and Nickel-Base Alloy Surface Alterations in Simulated Hot Corrosion Conditions with Emphasis on Eventual Application to Turbine Blade Corrosion. (SAR-2, Case Western Reserve Univ.; Grant NSG-3009) NASA CR-143173, 1975.

5. Stearns, Carl A.; Kohl, Fred J.; and Fryburg, George C.: Oxidative Vaporization Kinetics of Cr_2O_3 in Oxygen from 1000° to 1300° C. J. Electrochem. Soc., vol. 121, no. 7, July 1974, pp. 945-951.

6. Kvernes, Ingard A.; and Kofstad, Per: The Oxidation Behavior of Some Ni-Cr-Al Alloys at High Temperature. Met. Trans., vol. 3, no. 6, June 1972, pp. 1511-1519.

7. Garlick, Ralph G.; and Lowell, Carl E.: Alloy Composition Effects on Oxidation Products of VIA, B-1900, 713C, and 738X - A High Temperature Diffractometer Study. NASA TM X-2796, 1973.

8. Siegbahn, K.; et al.: ESCA (Electron Spectroscopy for Chemical Analysis): Atomic, Molecular, and Solid-State Structure Studied by Means of Electron Spectroscopy. Almquist & Wiksell (Sweden), 1967.

TABLE I. - COMPOSITION OF SUPERALLOYS

Element	Alloy							
	B-1900		NASA-TRW VIA		Alloy 713C		IN-738	
	Composition							
	wt %	at. %	wt %	at. %	wt %	at. %	wt %	at. %
Nickel	64.5	62.5	62	64.5	72	67	61.5	59
Chromium	8.0	8.7	6.1	7.1	12.5	13.2	16.0	17.5
Aluminum	6.0	12.6	5.4	12.2	6.1	12.4	3.4	7.2
Titanium	1.0	1.2	1.0	1.3	.8	.9	3.4	4.0
Cobalt	10.0	9.6	7.5	7.7	------	-----	8.5	8.2
Molybdenum	6.0	3.5	2.0	1.3	4.2	2.4	1.7	1.0
Tungsten	[a].1	-----	5.5	1.8	------	-----	2.6	.8
Tantalum	4.3	1.4	9.0	3.0	------	-----	1.7	.6
Niobium	[a].1	-----	.5	.3	2.0	1.2	.9	.6
Hafnium	------	-----	.4	.1	------	-----	-----	-----
Zirconium	.08	-----	-----	----	------	-----	.1	.06
Rhenium	------	-----	.3	.1	------	-----	-----	-----
Iron	[a].35	-----	-----	-----	[a]2.5	[a]2.5	[a].5	-----
Carbon	.1	.47	.13	.66	.12	.55	.17	.81
Boron	.015	-----	-----	-----	[a].012	-----	.01	-----
Silicon	[a].25	-----	-----	-----	[a].5	-----	[a].3	-----
Manganese	[a].2	-----	-----	-----	[a].25	-----	[a].2	-----

[a]Maximum value.

TABLE II. - PARABOLIC RATE CONSTANTS FOR OXIDATION IN 1 ATMOSPHERE OF SLOWLY FLOWING OXYGEN

Alloy	Temperature, °C	Time range, hr	Parabolic rate constant, $mg^2\ cm^{-4}\ hr^{-1}$
Alloy 713C	900	2 - 50	0.0127
	1000	------	(a)
IN-738	900	1 - 100	0.025
	1000	1 - 50	.288

[a]No fit.

TABLE III. - THICKNESS OF OXIDE SCALE REGIONS AND OF γ' DEPLETION ZONE ON OXIDIZED SPECIMENS

Alloy	Temperature, °C	Thickness of oxide layer, μm	Thickness[a] of internal oxidation zone, μm	Thickness[a] of γ' depletion zone, μm
B-1900	900	~1.5	2 - 5	2 - 7
	1000	~2	-----	3 - 7
NASA-TRW VIA	900	~2	2 - 5	2 - 10
	1000	~2	-----	5 - 10
Alloy 713C	900	~3	5 - 8	15 - 20
	1000	2 - 10	-----	7 - 15
IN-738	900	8 - 12	~20	~25
	1000	~20	~30	~50

[a]Thickness measured from inner surface of the continuous oxide scale.

TABLE IV. - PHASES IDENTIFIED BY X-RAY DIFFRACTION AND OXIDIZED ELEMENTS DETECTED BY ESCA ON SAMPLES OXIDIZED FOR 100 HOURS IN 1 ATMOSPHERE OF SLOWLY FLOWING OXYGEN

Alloy	Temperature, °C	Phases identified by X-ray diffraction[a, b]	Oxidized elements detected by ESCA[c], at. %
B-1900	900	Tapiolite (W+) Mixed spinels (8.15×10^{-10} m) (VW) α-Al_2O_3 (VVW) Cr_2O_3 (VVW)	51 Al, 14 Cr, 12 Ti, 8 Ni, 6.5 Co, 6 Mo, 1 Ta
	1000	α-Al_2O_3 (W) Tapiolite (VW)	79 Al, 7.7 Ti, 3.8 Cr, 2.7 Ta, 2.2 Mo, 2.2 Co, 2 Ni
NASA-TRW VIA	900	Tapiolite (M) Mixed spinels (8.15×10^{-10} m) (VW) α-Al_2O_3 (VVW)	52 Al, 17.5 Ti, 14.5 Cr, 12 Ni, 2.5 Co, 1.5 Mo, 0.5 Ta
	1000	Tapiolite (W+) α-Al_2O_3 (W) Al spinel (8.05×10^{-10} m) (VW) Cr spinel (8.30×10^{-10} m) (VW)	80.7 Al, 6.3 Cr, 5.0 Ti, 3.1 Ni, 3 Ta, 1.9 Co
Alloy 713C	900	Cr_2O_3 (M)	40 Cr, 23 Ti, 15 Al, 15 Ni, 3.5 Mo, 2 Nb
	1000	Cr spinel (8.30×10^{-10} m) (M) α-Al_2O_3 (W) Cr_2O_3 (W) Tapiolite (VVW)	54.5 Cr, 31 Al, 10 Ti, 2.5 Ni, 1.5 Nb
IN-738	900	Cr_2O_3 (S) TiO_2 (M)	58 Ti, 26 Cr, 7 Al, 5 Ni; 2.5 Co, 1 Ta
	1000	Cr_2O_3 (VS) TiO_2 (S) Tapiolite (VVW)	50 Ti, 30 Cr, 17 Al, 3 Ni, 1 Nb, 1 Mo, 1 Ta

[a]Phases listed in order of decreasing intensity of diffraction pattern. The pattern characteristic of the nickel alloy solid-solution phase was also observed for all samples, revealing that the X-rays had penetrated through the oxide scale.

[b]Symbols indicate a qualitative measure of diffraction pattern intensity, which is a function not only of the oxide composition but also of oxide thickness: V ≡ very, S ≡ strong, M ≡ medium, W ≡ weak.

[c]Atomic percent composition estimated by a tentative quantitative treatment of the ESCA data. See ref. 4 for details. The oxidation states were determined to be Ni^{+2}, Co^{+2}, Al^{+3}, Cr^{+3}, Ti^{+4}, Ta^{+5}, Nb^{+5}, Mo^{+6}, and W^{+6}.

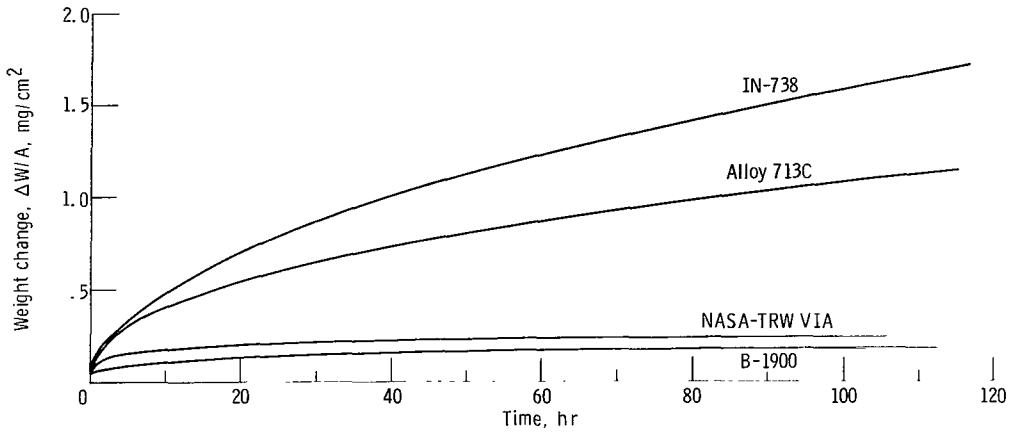

Figure 1. - Rate of oxidation of alloys at 900° C in 1 atmosphere of slowly flowing oxygen.

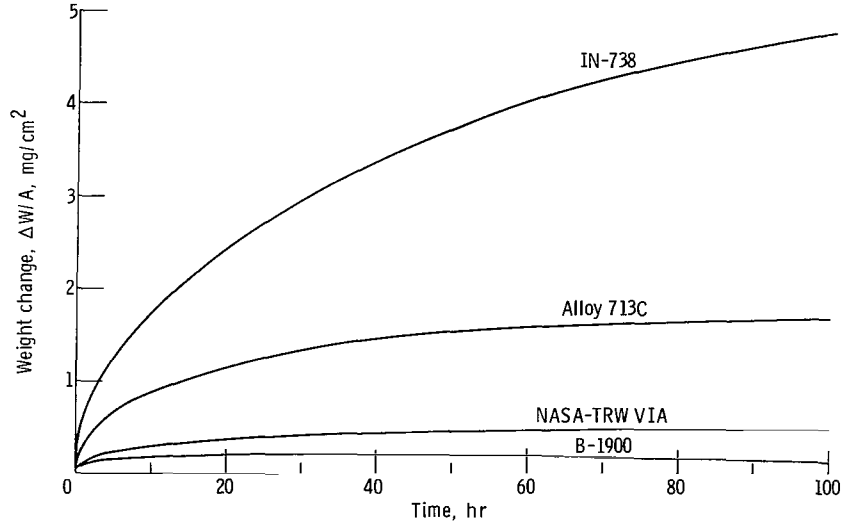

Figure 2. - Rate of oxidation of alloys at 1000° C in 1 atmosphere of slowly flowing oxygen.

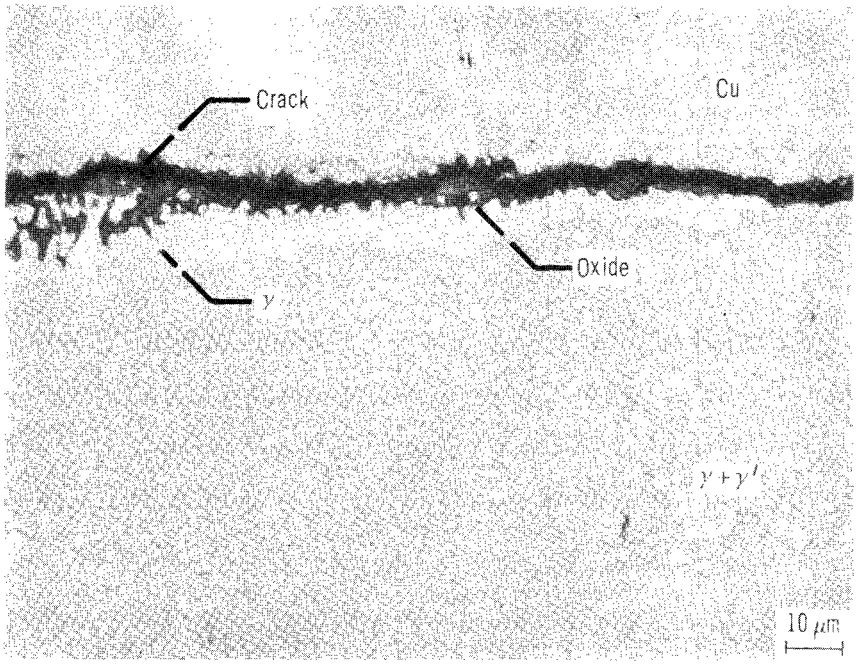

(a) Temperature, 900° C.

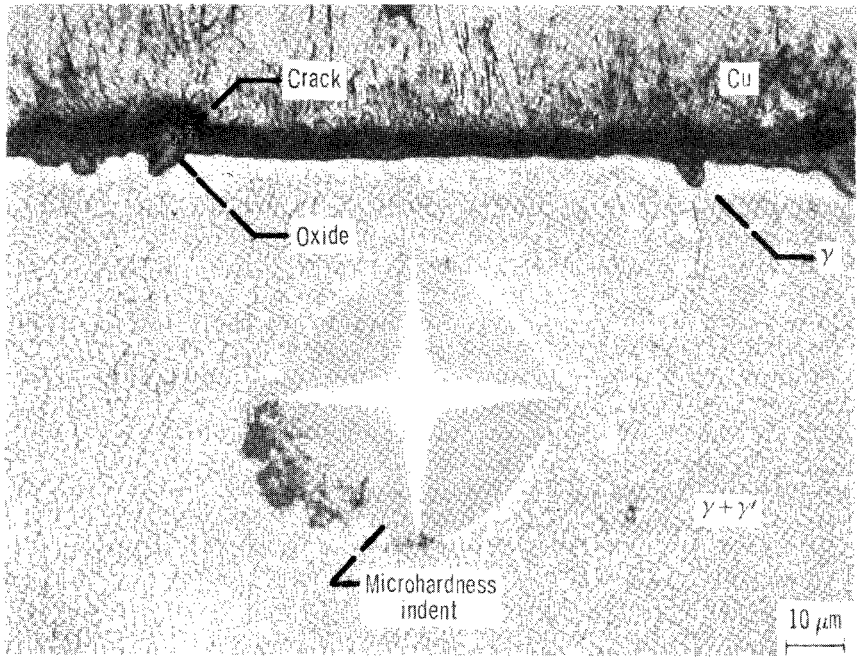

(b) Temperature, 1000° C.

Figure 3. - Light micrograph of cross section of oxide scale on B-1900.

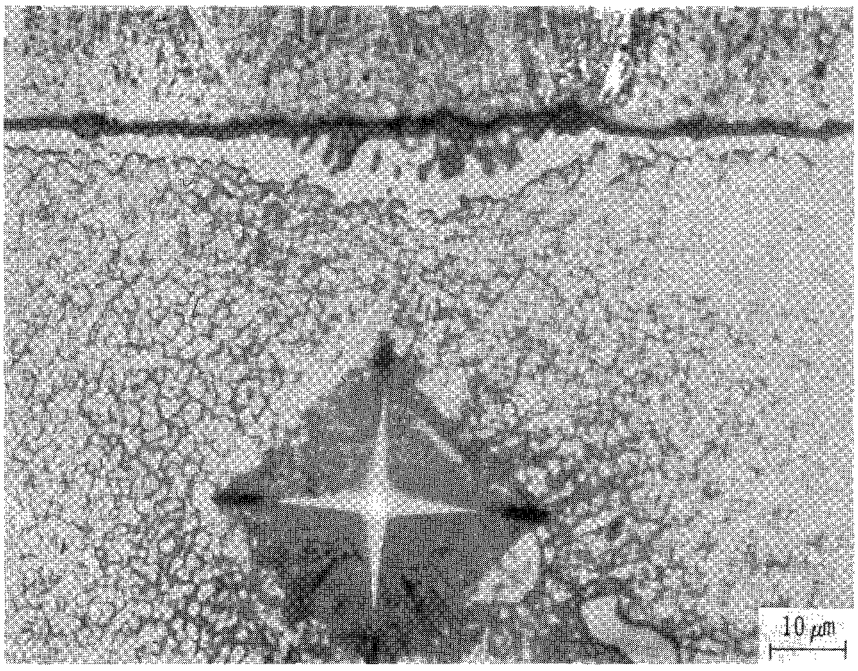

(a) Temperature, 900° C.

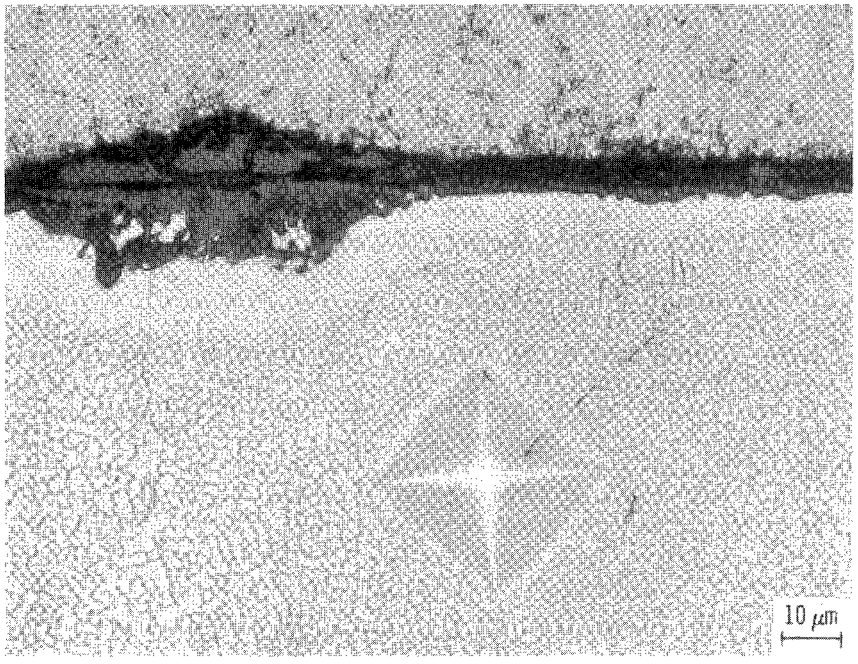

(b) Temperature, 1000° C.

Figure 4. - Light micrograph of cross section of oxide scale on NASA-TRW VIA.

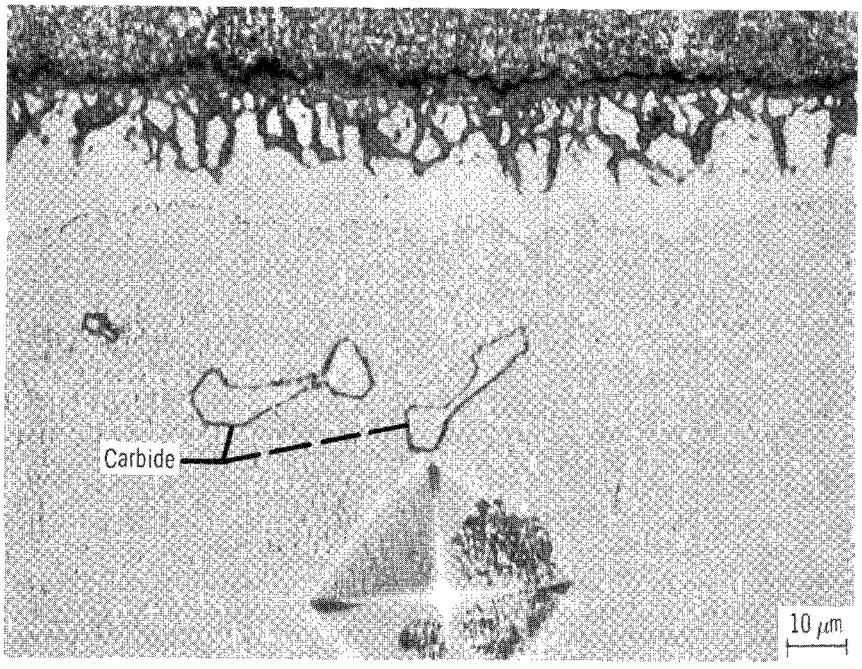

(a) Temperature, 900° C.

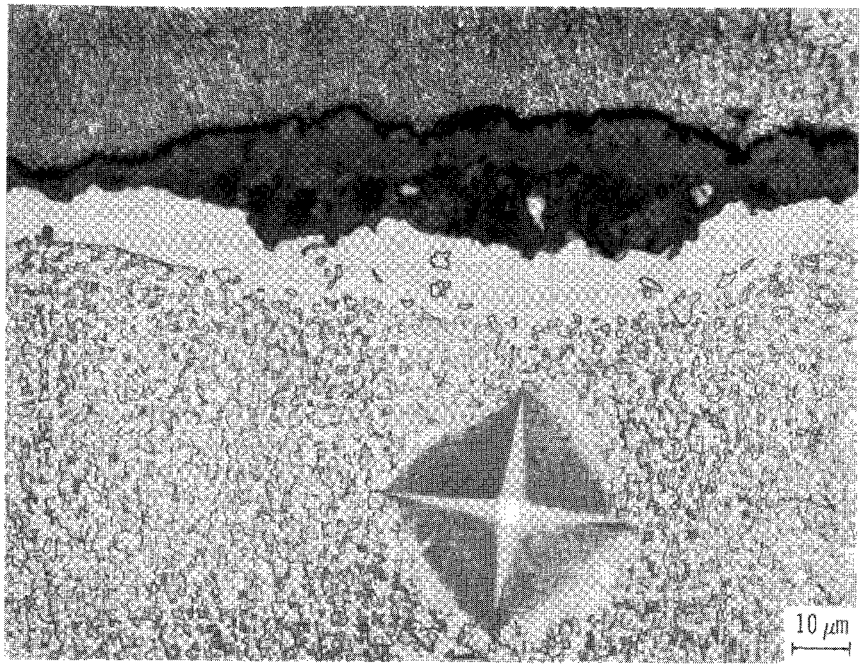

(b) Temperature, 1000° C.

Figure 5. - Light micrograph of cross section of oxide scale on alloy 713C.

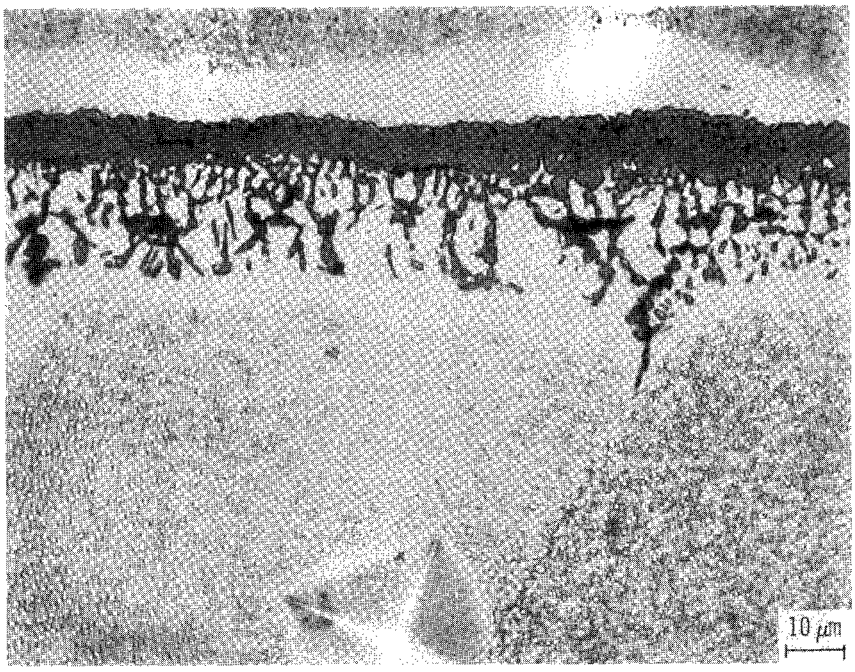

(a) Temperature, 900° C.

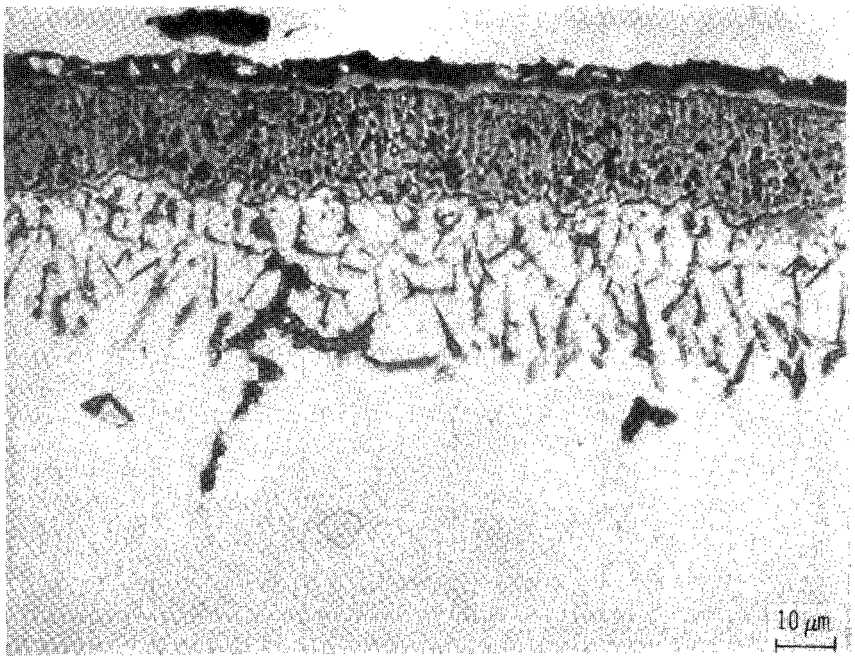

(b) Temperature, 1000° C.

Figure 6. - Light micrograph of cross section of oxide scale on IN-738.

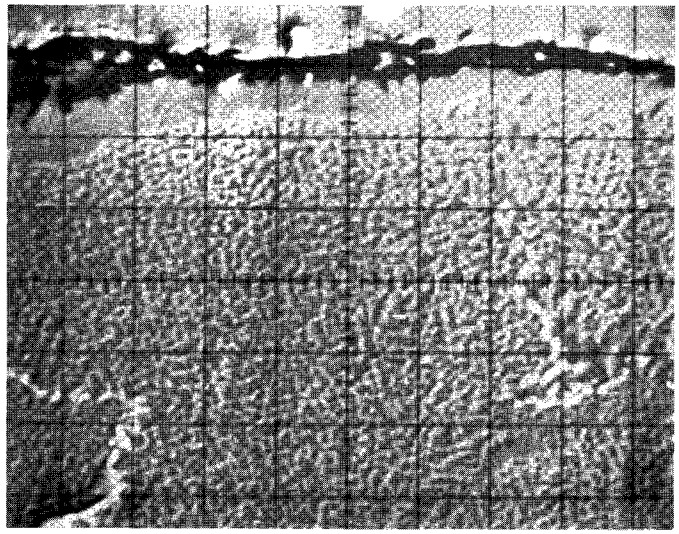

(a) Backscattered electron micrograph.

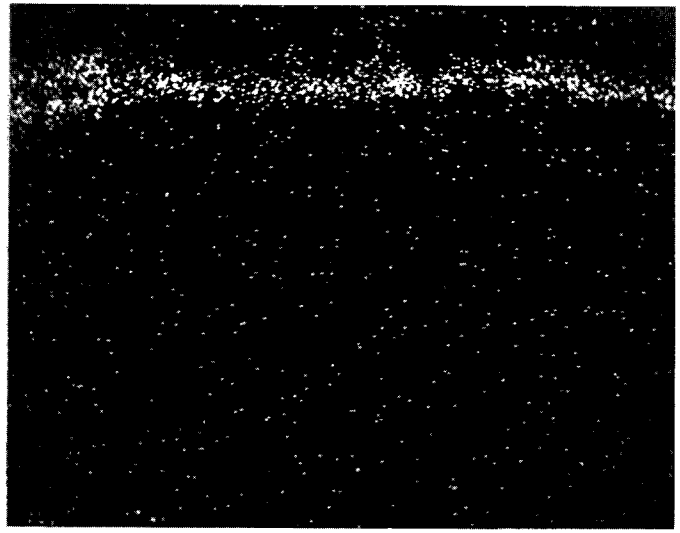

(b) Oxygen.

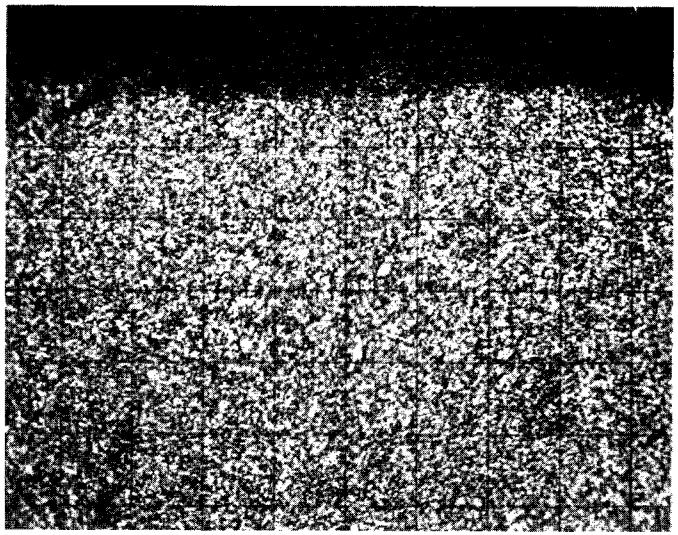

(c) Nickel.

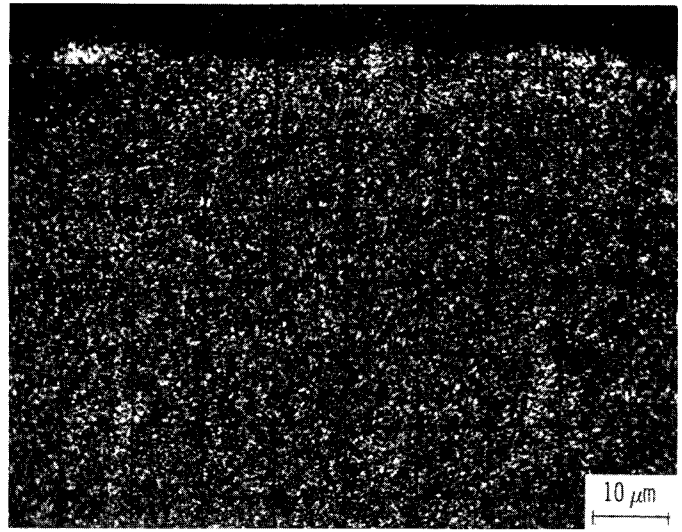

(d) Chromium.

Figure 7. - Electron and elemental X-ray micrographs of cross section of oxide formed on B-1900 at 900° C after 100 hours in slowly flowing oxygen.

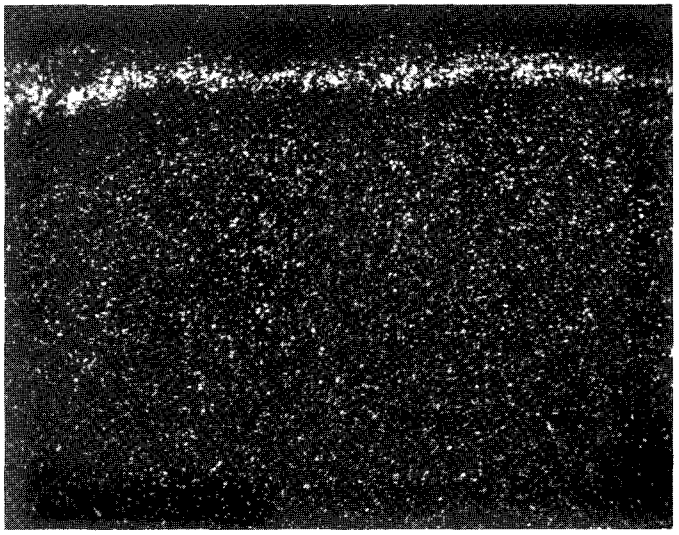

(e) Aluminum.

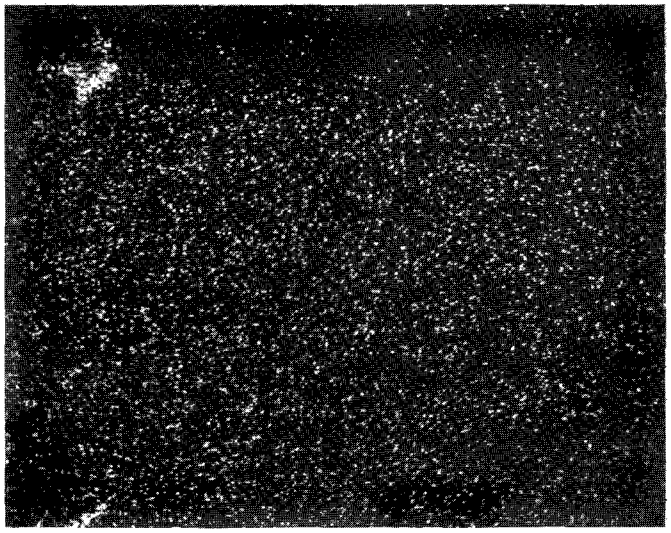

(f) Tantalum.

(g) Titanium.

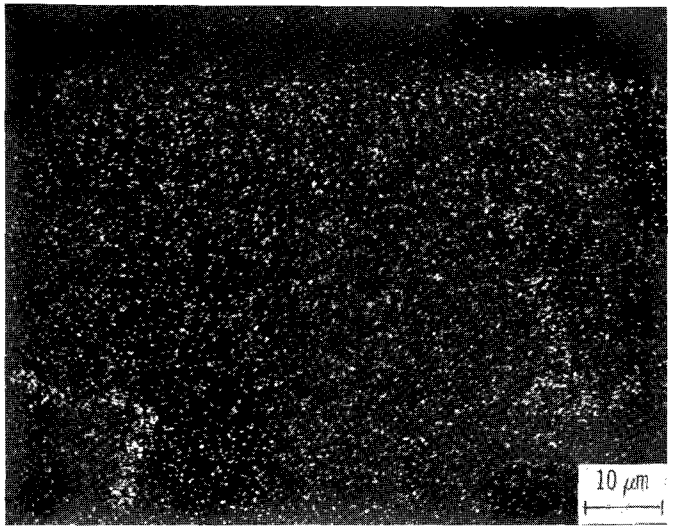

(h) Molybdenum.

Figure 7. - Concluded.

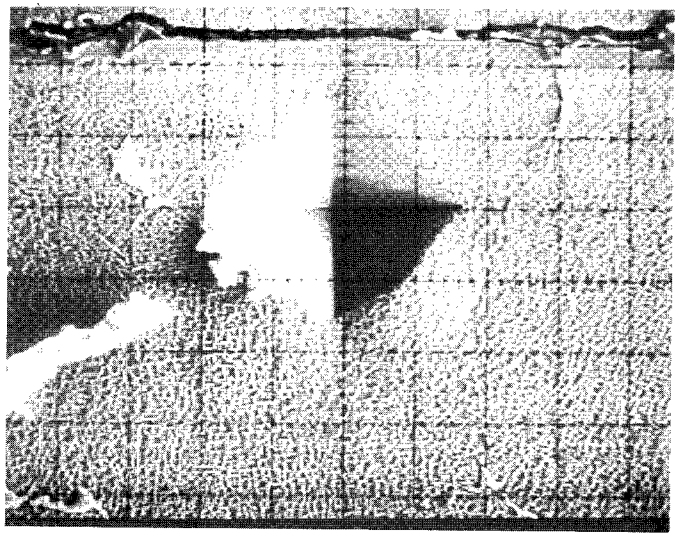

(a) Backscattered electron micrograph.

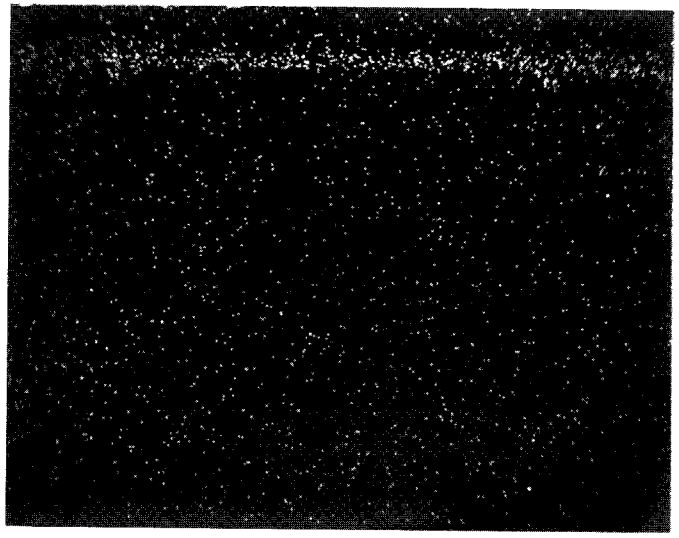

(b) Oxygen.

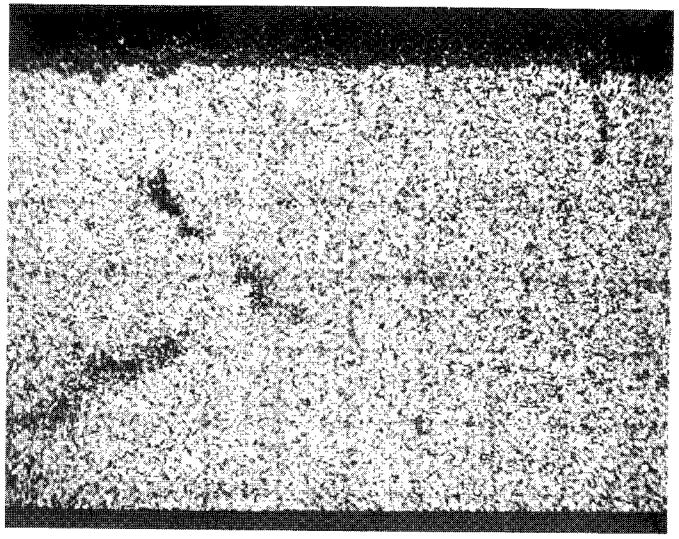

(c) Nickel.

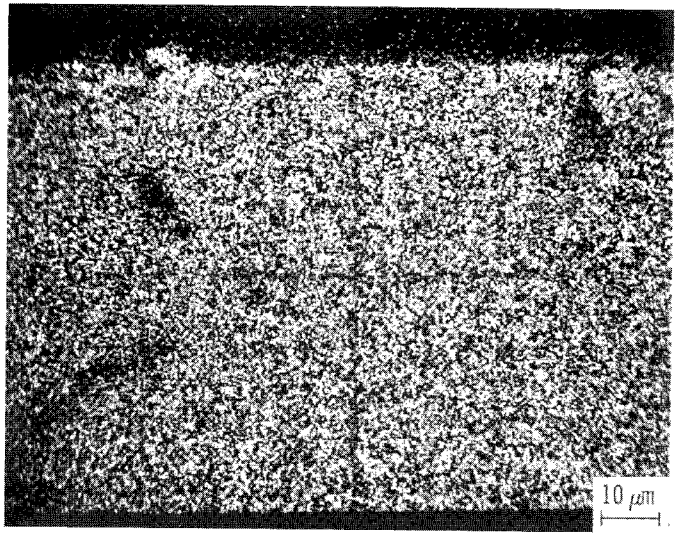

(d) Chromium.

Figure 8. - Electron and elemental X-ray micrographs of cross section of oxide formed on B-1900 at 1000° C after 100 hours in slowly flowing oxygen.

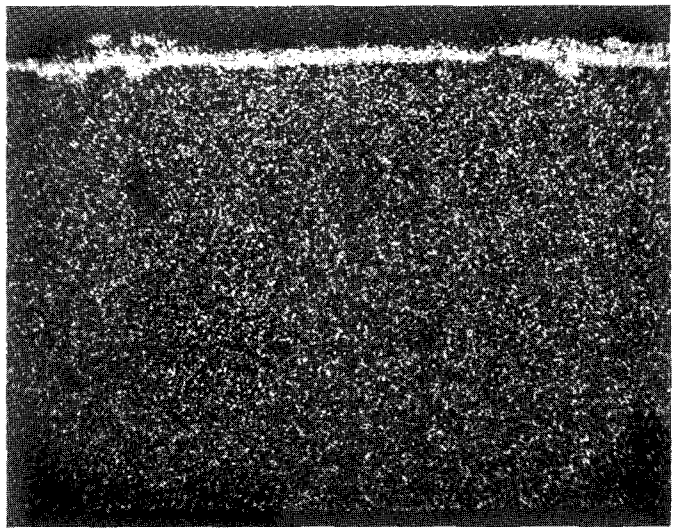

(e) Aluminum.

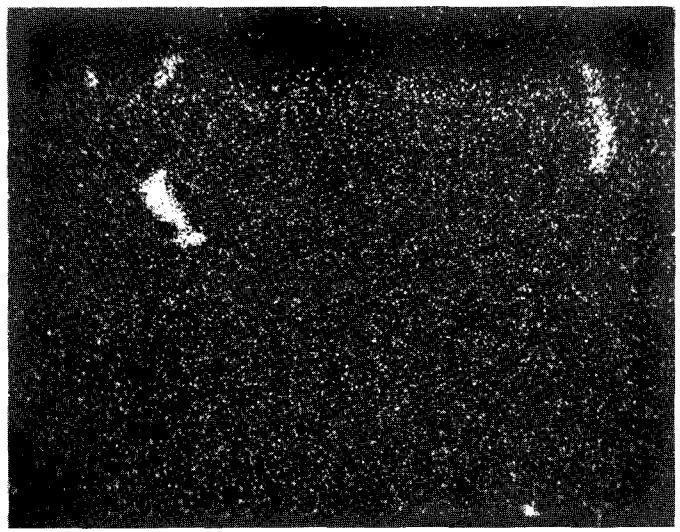

(f) Tantalum.

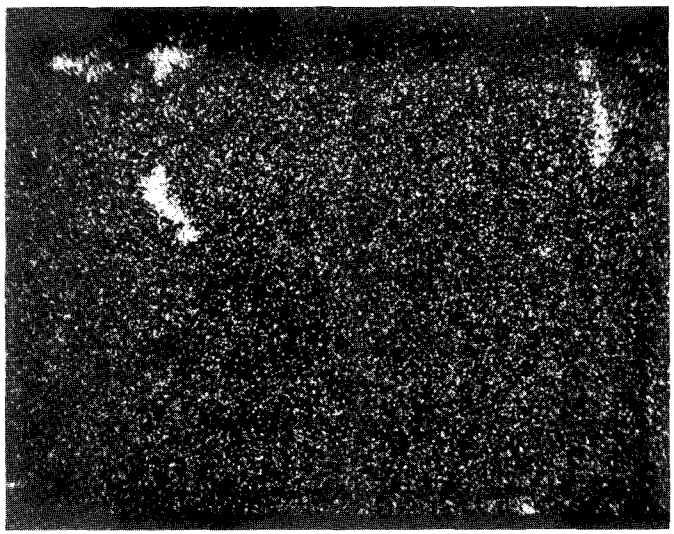

(g) Titanium.

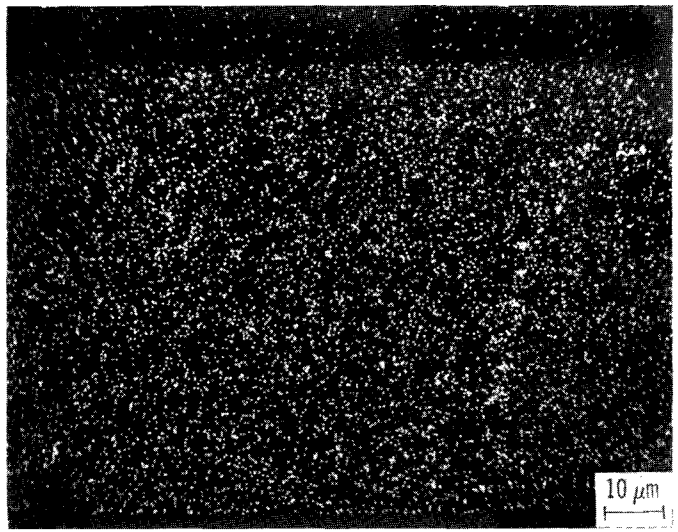

(h) Molybdenum.

Figure 8. - Concluded.

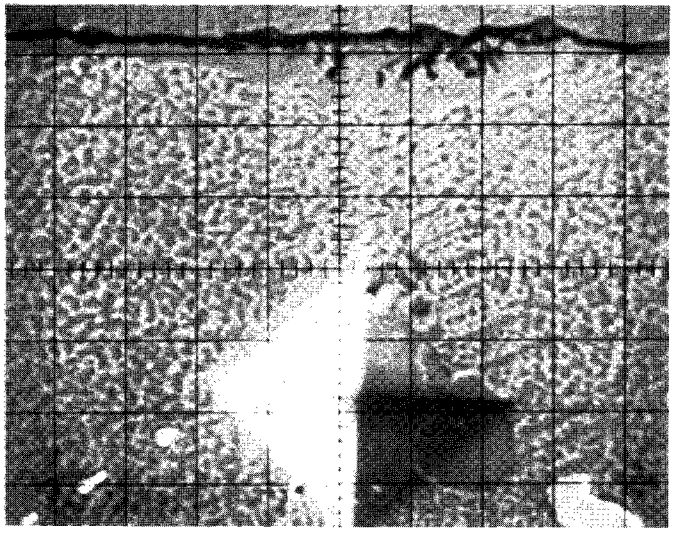

(a) Backscattered electron micrograph.

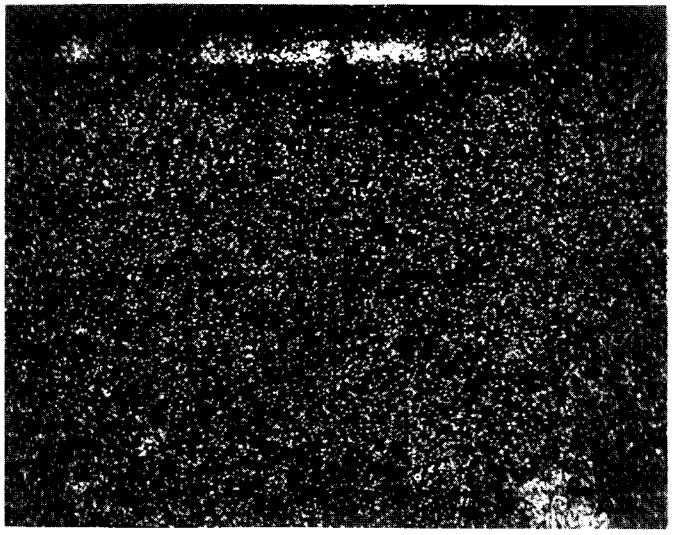

(b) Oxygen.

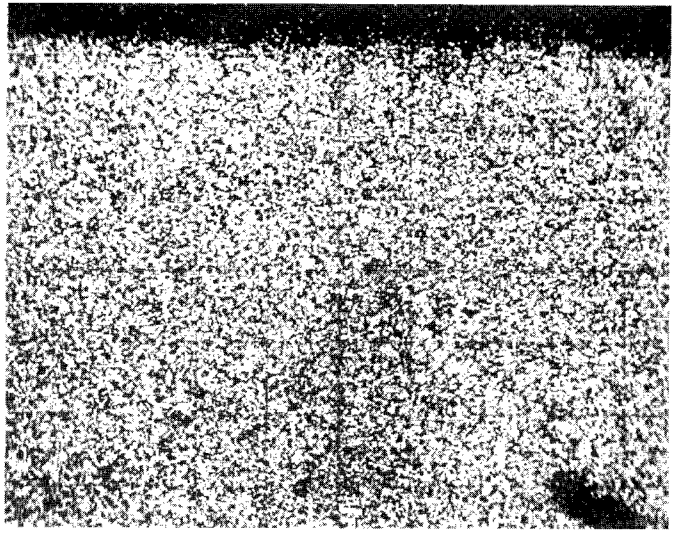

(c) Nickel.

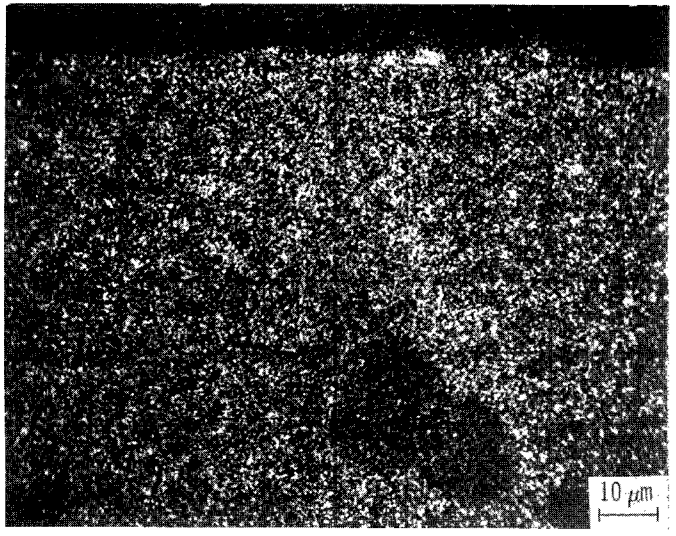

(d) Chromium.

Figure 9. - Electron and elemental X-ray micrographs of cross section of oxide formed on NASA-TRW VIA at 900° C after 100 hours in slowly flowing oxygen.

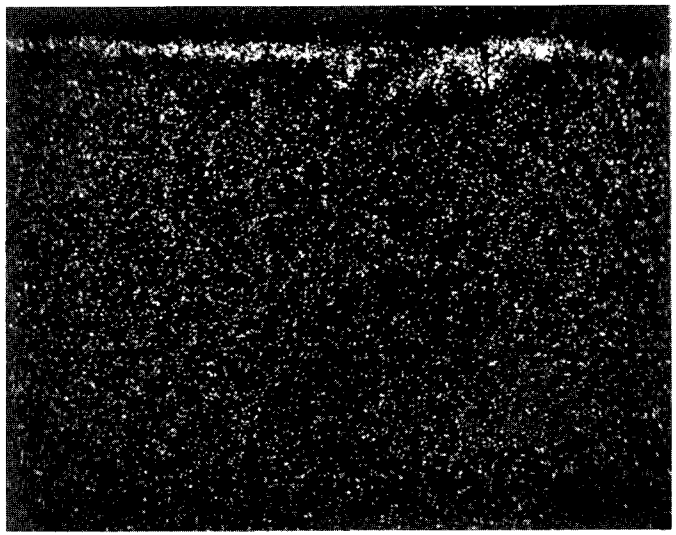

(e) Aluminum.

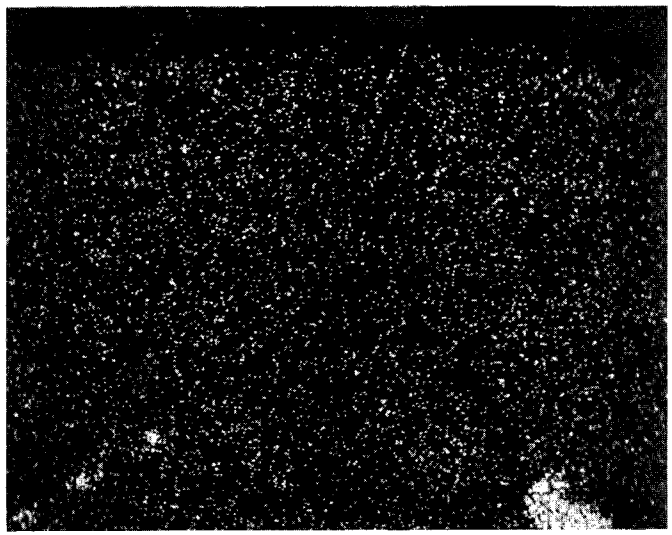

(f) Tantalum.

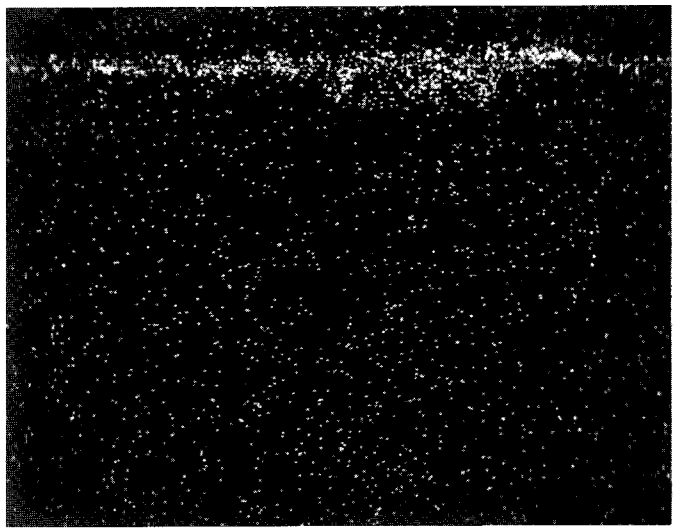

(g) Titanium.

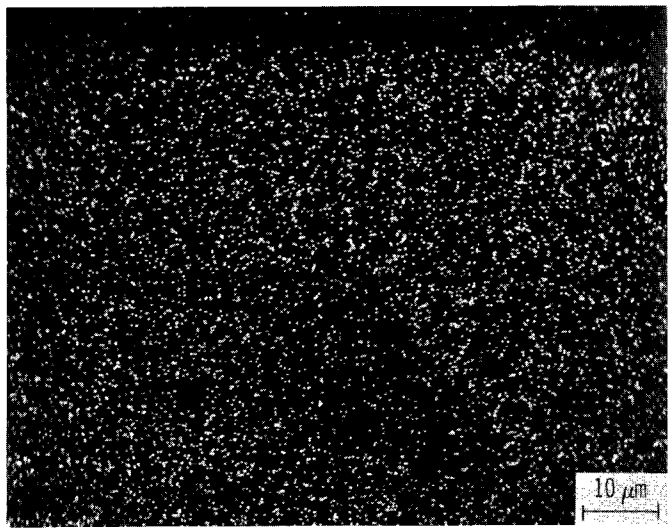

(h) Tungsten.

Figure 9. - Concluded.

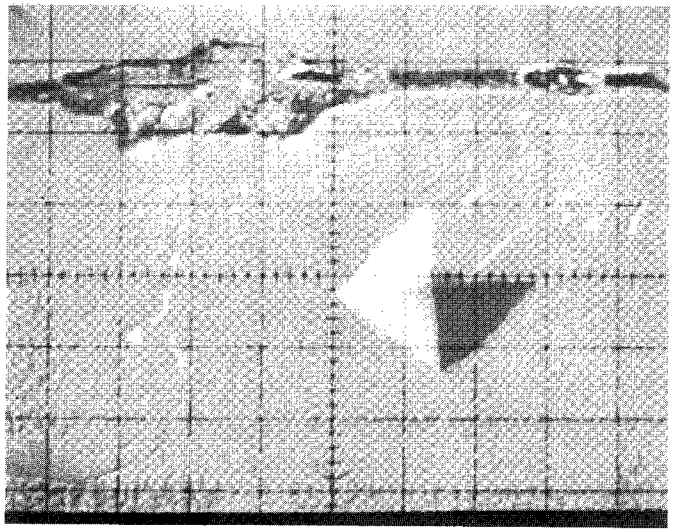

(a) Backscattered electron micrograph.

(b) Oxygen.

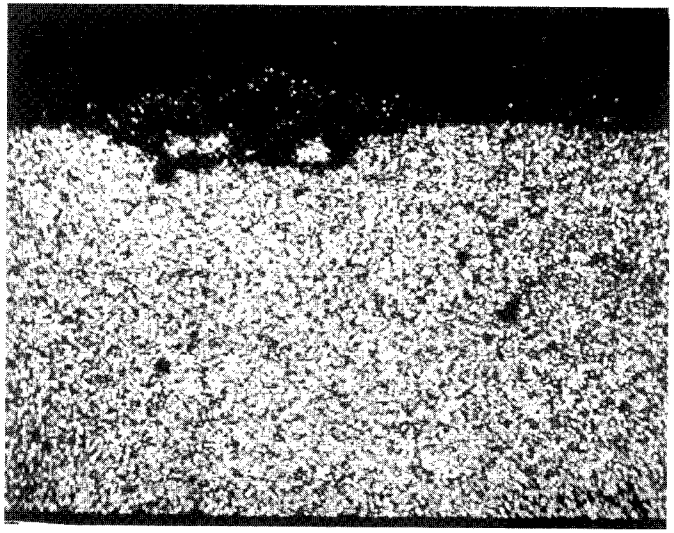

(c) Nickel.

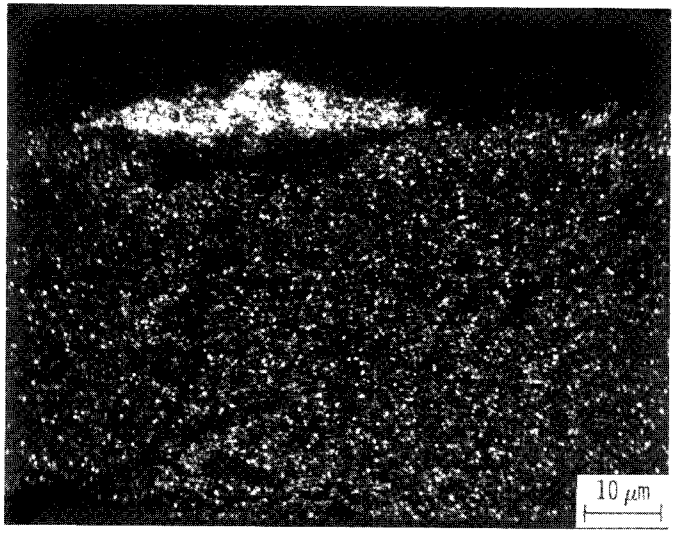

(d) Chromium.

Figure 10. - Electron and elemental X-ray micrographs of cross section of oxide formed on NASA-TRW VIA at 1000° C after 100 hours in slowly flowing oxygen.

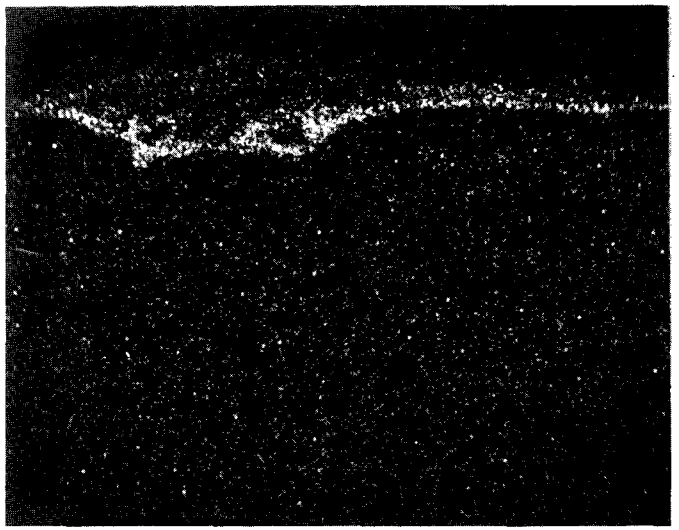

(e) Aluminum.

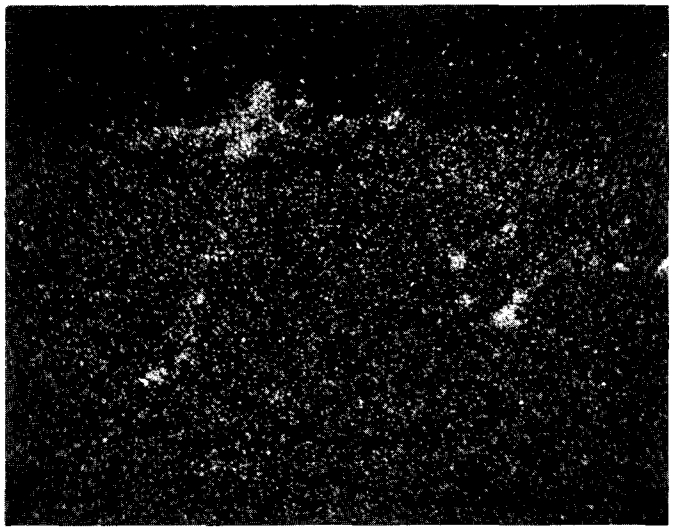

(f) Tantalum.

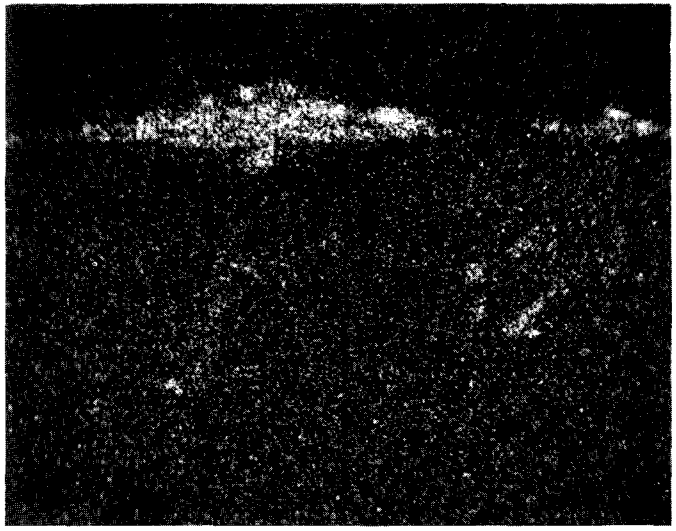

(g) Titanium.

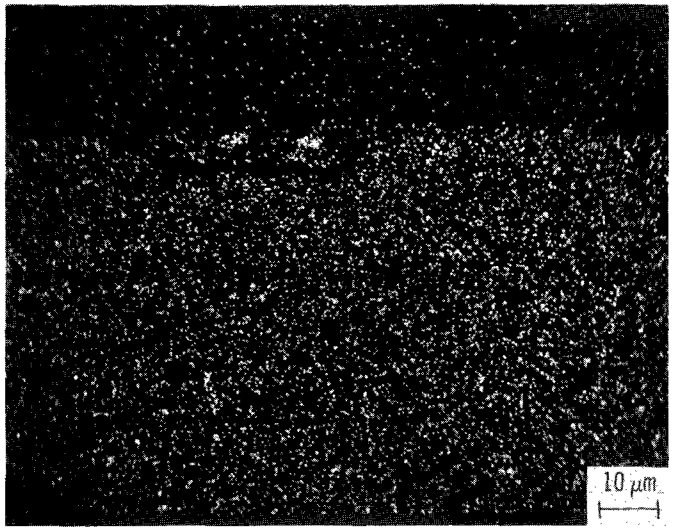

(h) Tungsten.

Figure 10. - Concluded.

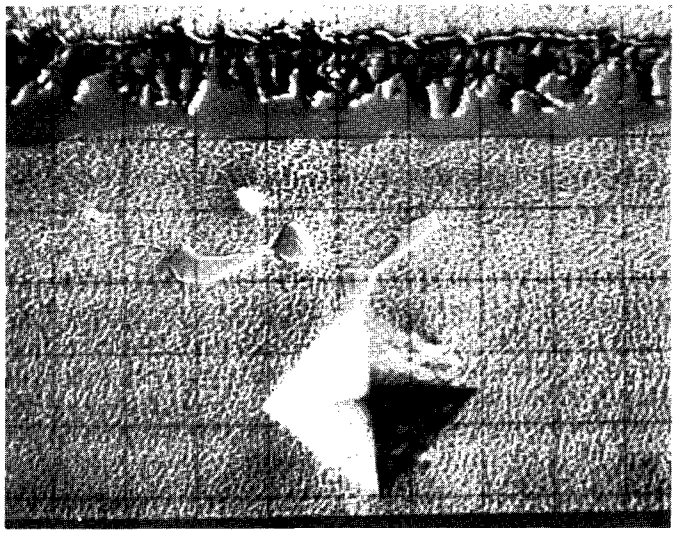

(a) Backscattered electron micrograph.

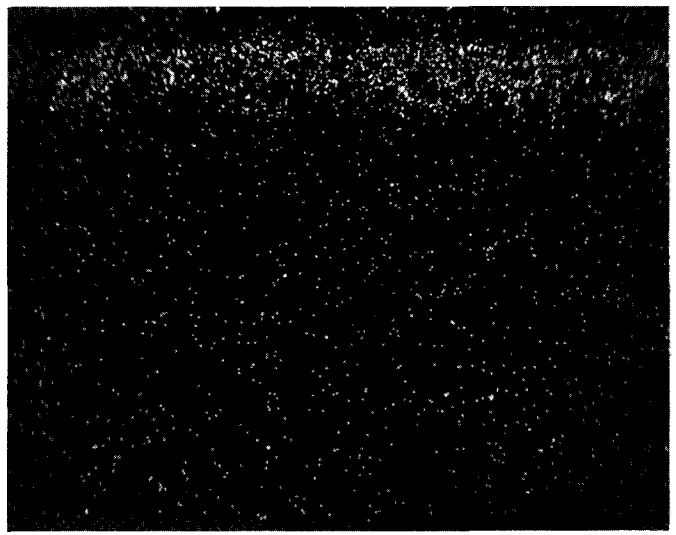

(b) Oxygen.

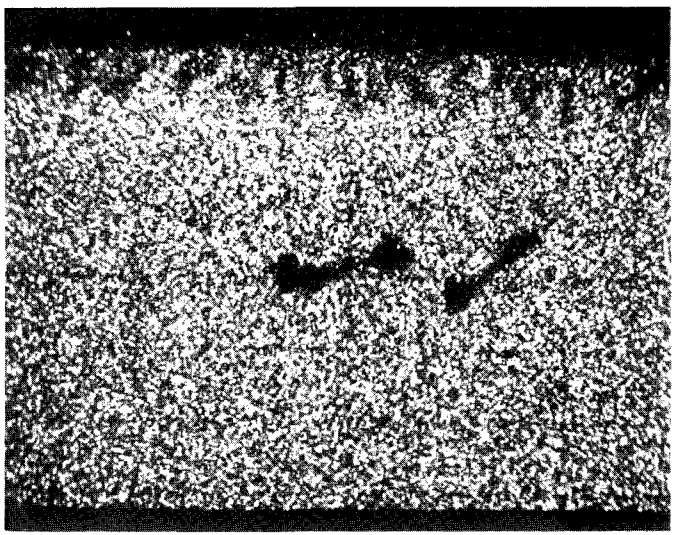

(c) Nickel.

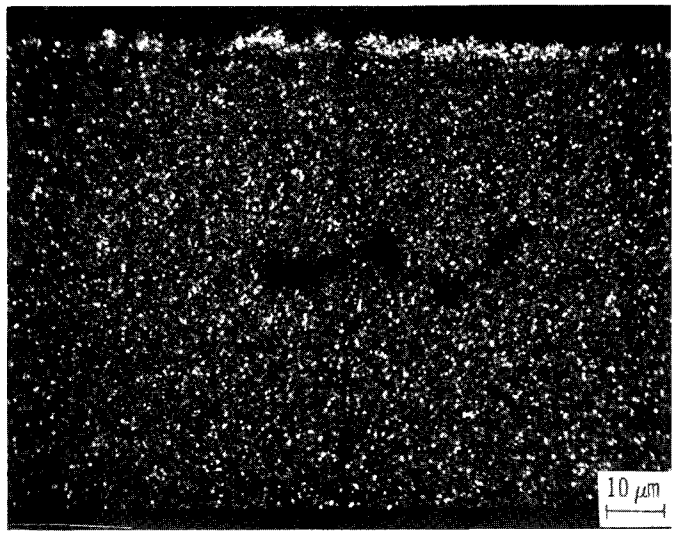

(d) Chromium.

Figure 11. - Electron and elemental X-ray micrographs of cross section of oxide formed on alloy 713C at 900° C after 100 hours in slowly flowing oxygen.

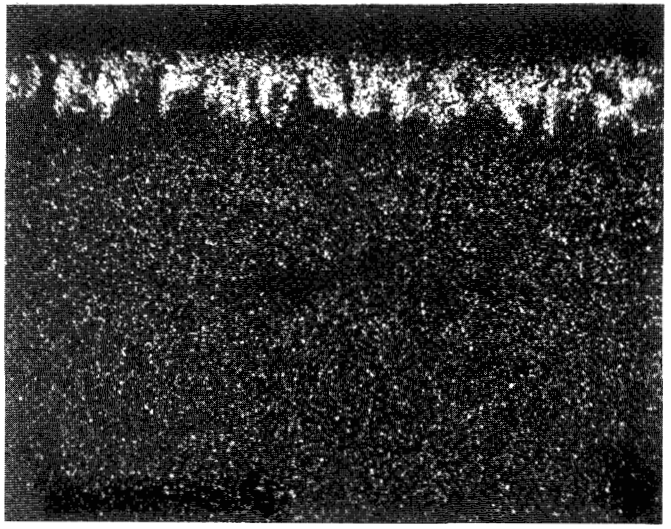

(e) Aluminum.

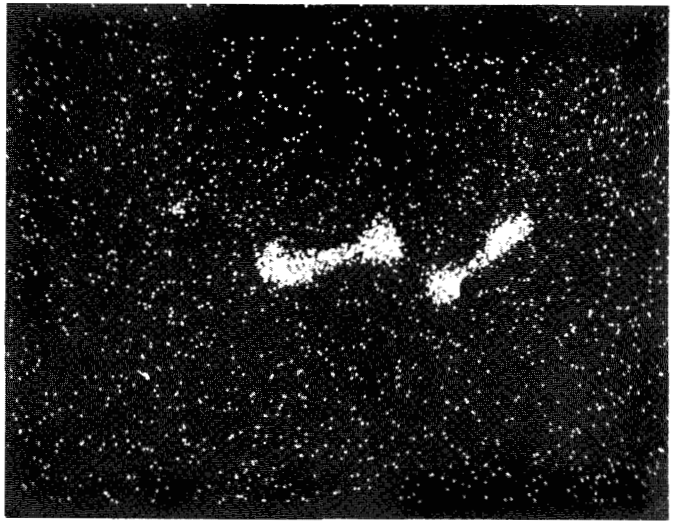

(f) Niobium.

(g) Titanium.

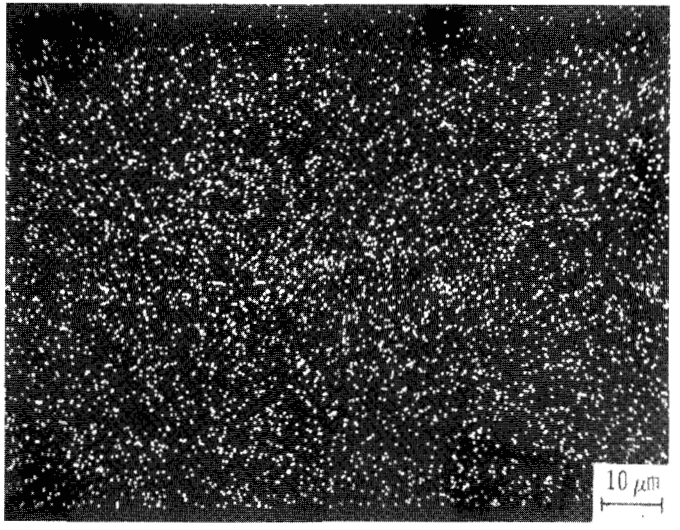

(h) Molybdenum.

Figure 11. - Concluded.

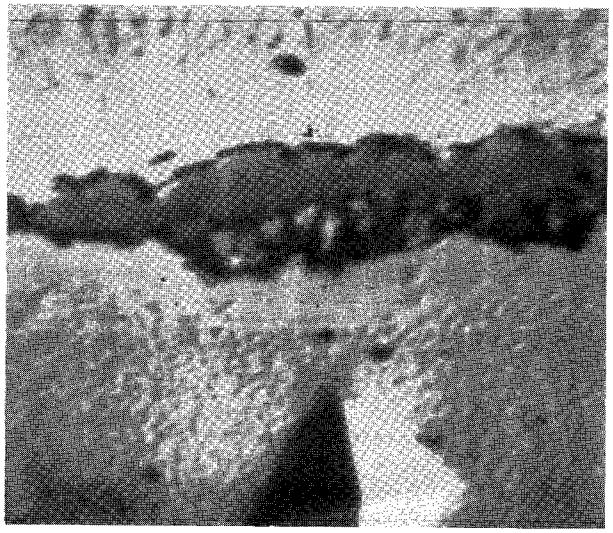

(a) Backscattered electron micrograph.

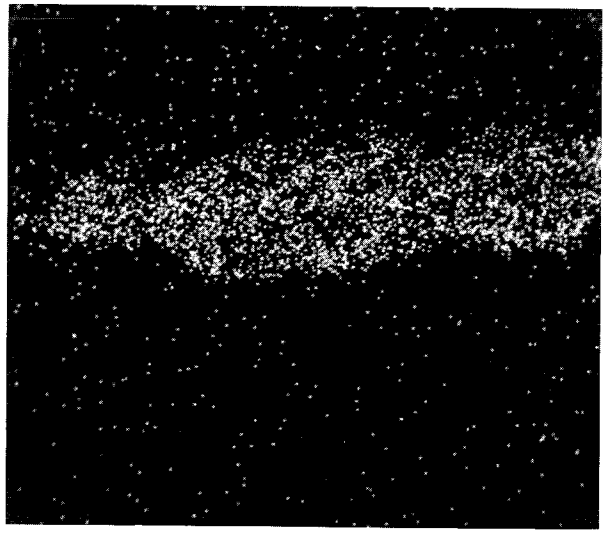

(b) Oxygen.

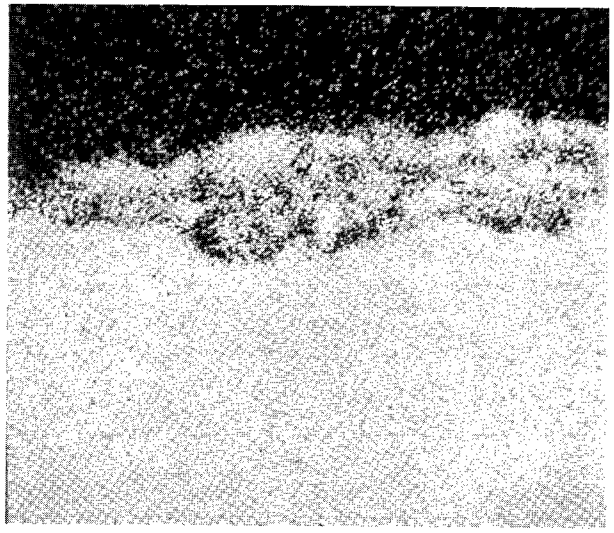

(c) Nickel.

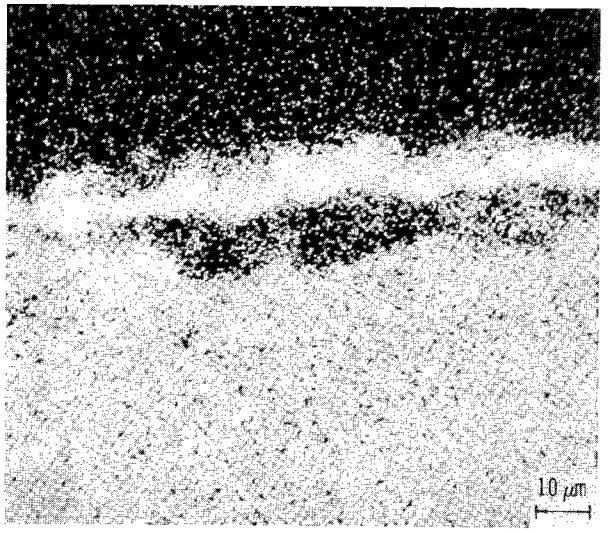

(d) Chromium.

Figure 12. - Electron and elemental X-ray micrographs of cross section of oxide formed on alloy 713C at 1000° C after 100 hours in slowly flowing oxygen.

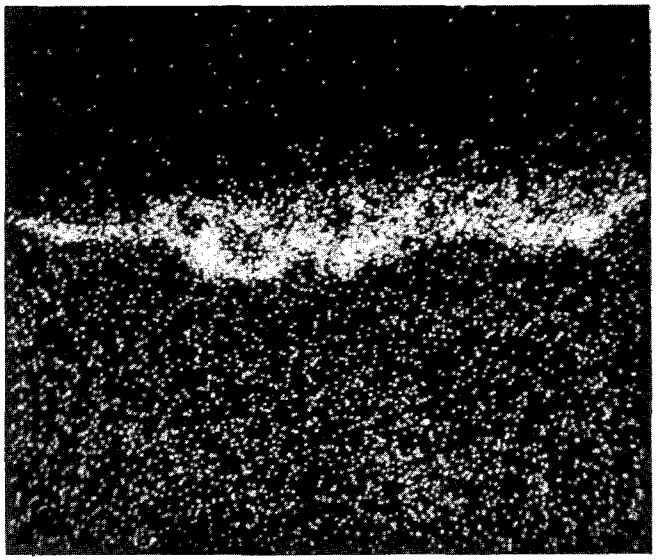

(e) Aluminum.

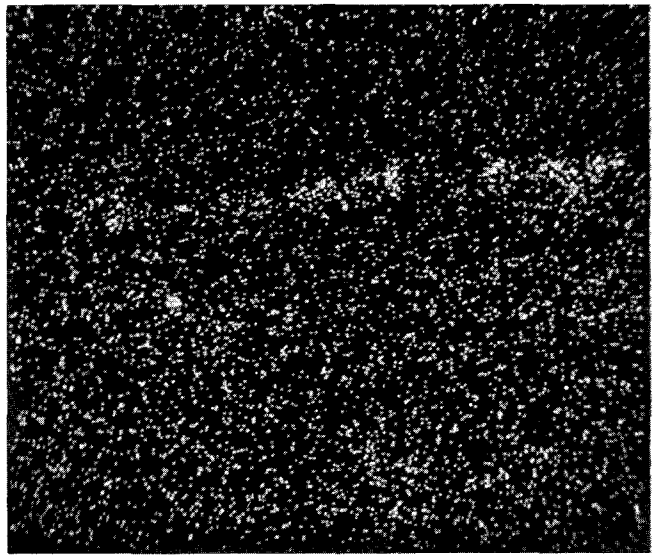

(f) Niobium.

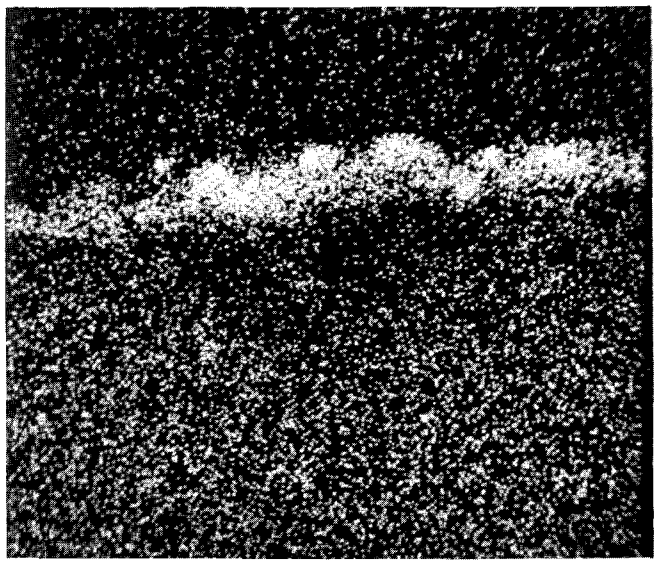

(g) Titanium.

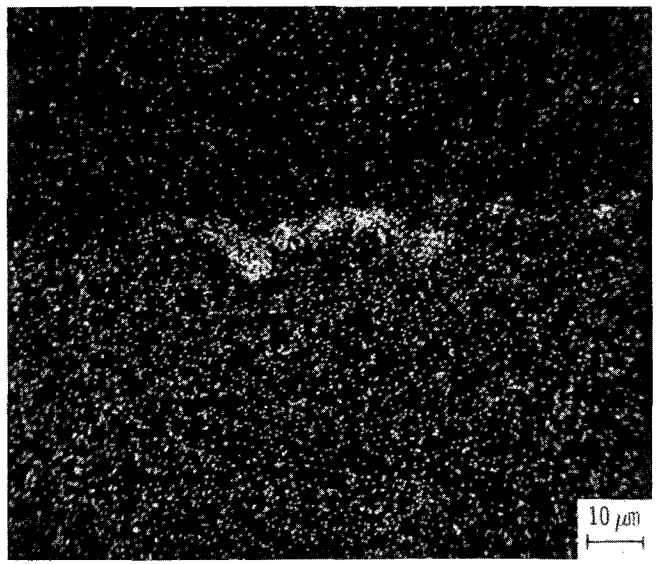

(h) Molybdenum.

Figure 12. - Concluded.

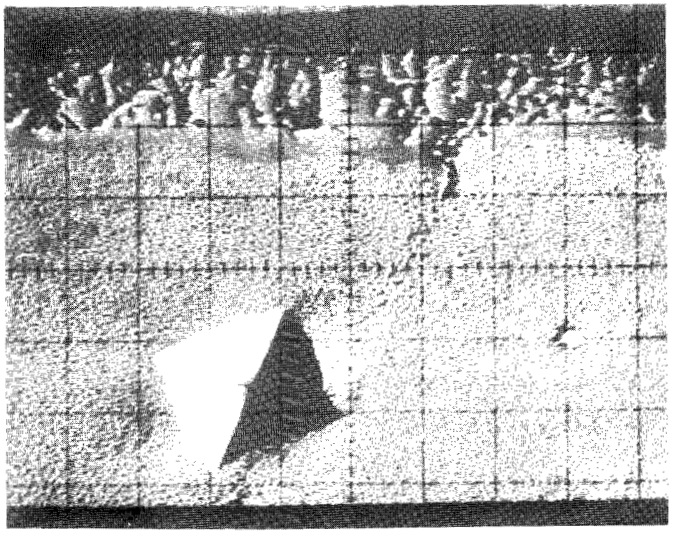

(a) Backscattered electron micrograph.

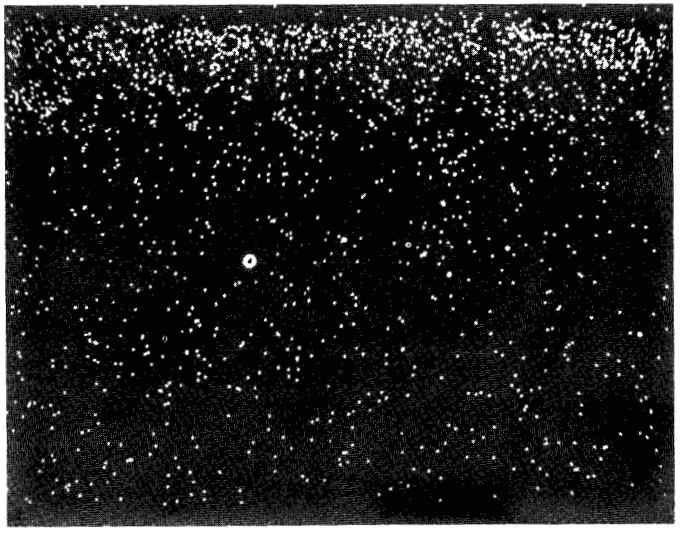

(b) Oxygen.

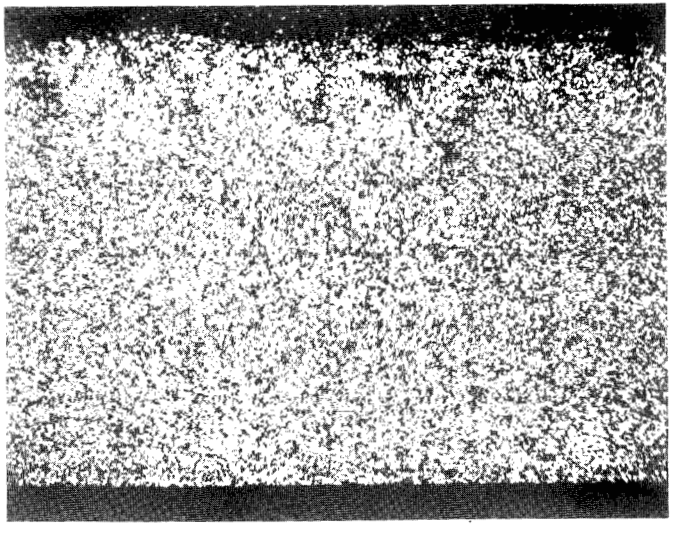

(c) Niobium.

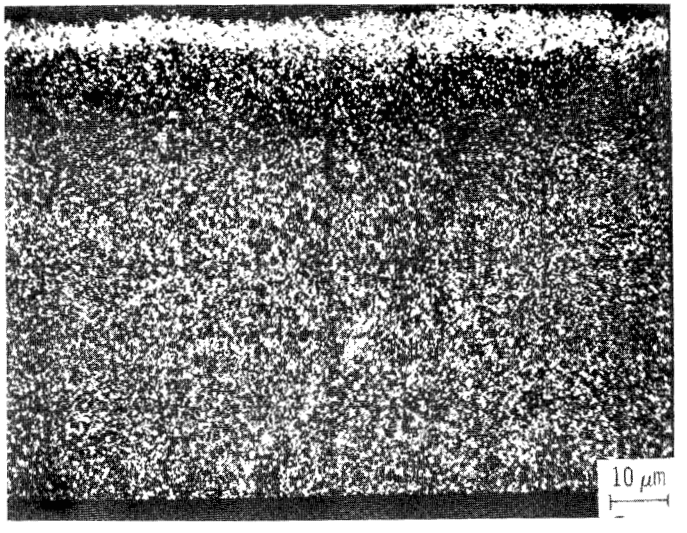

(d) Chromium.

Figure 13. - Electron and elemental X-ray micrographs of cross section of oxide formed on IN-738 at 900° C after 100 hours in slowly flowing oxygen.

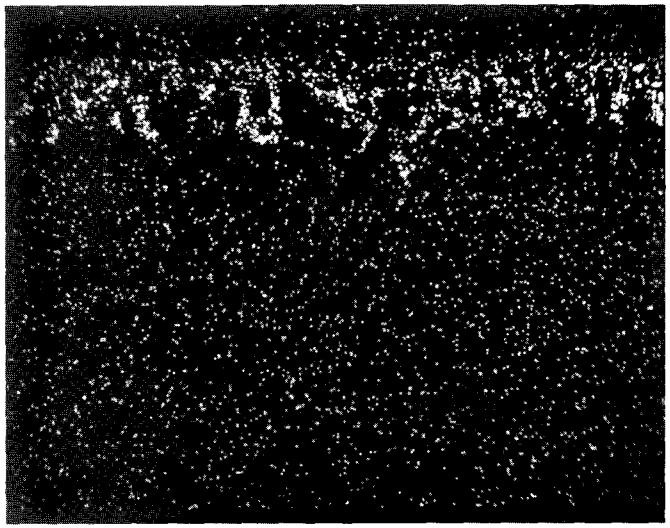

(e) Aluminum.

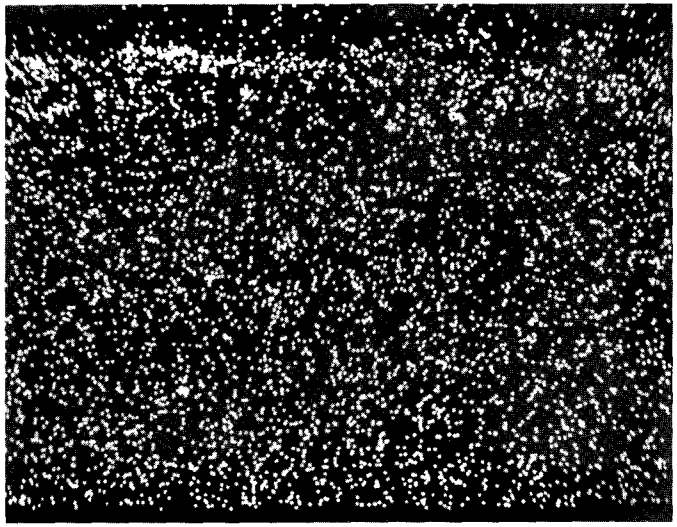

(f) Tantalum.

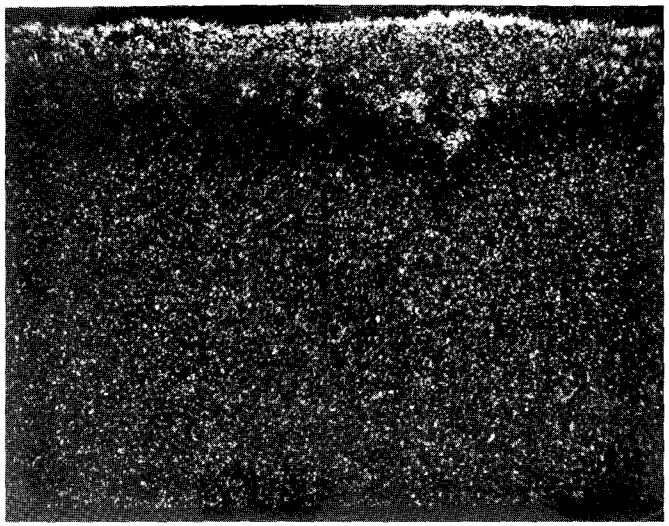

(g) Titanium.

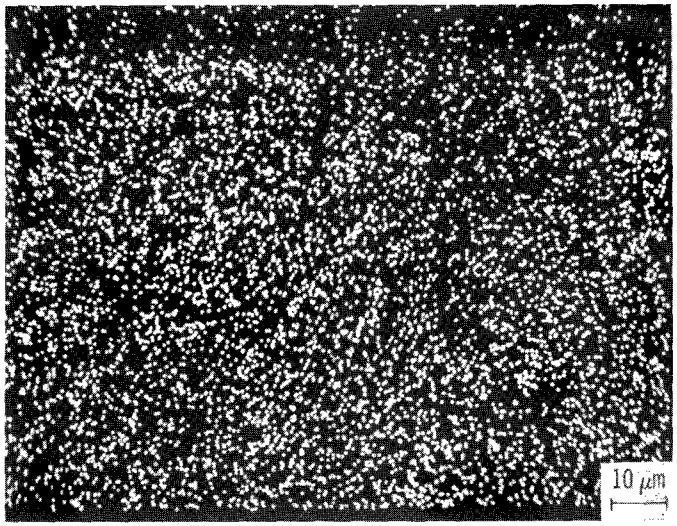

(h) Tungsten.

Figure 13. - Concluded.

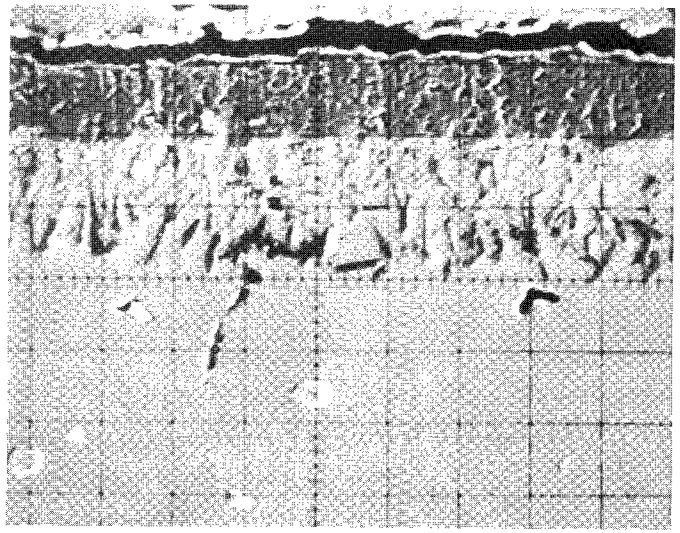

(a) Backscattered electron micrograph.

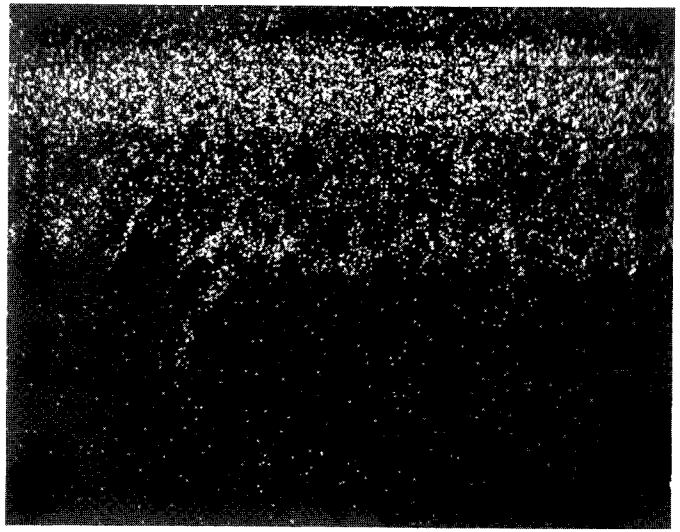

(b) Oxygen.

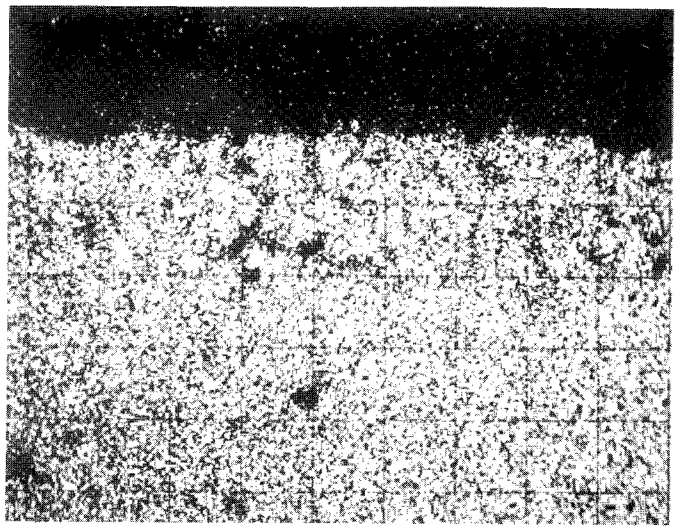

(c) Niobium.

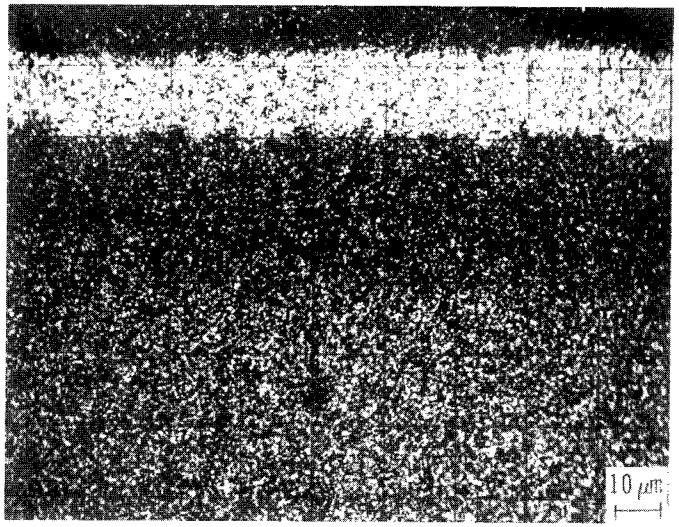

(d) Chromium.

Figure 14. - Electron and elemental X-ray micrographs of cross section of oxide formed on IN-738 at 1000° C after 100 hours in slowly flowing oxygen.

(e) Aluminum.

(f) Tantalum.

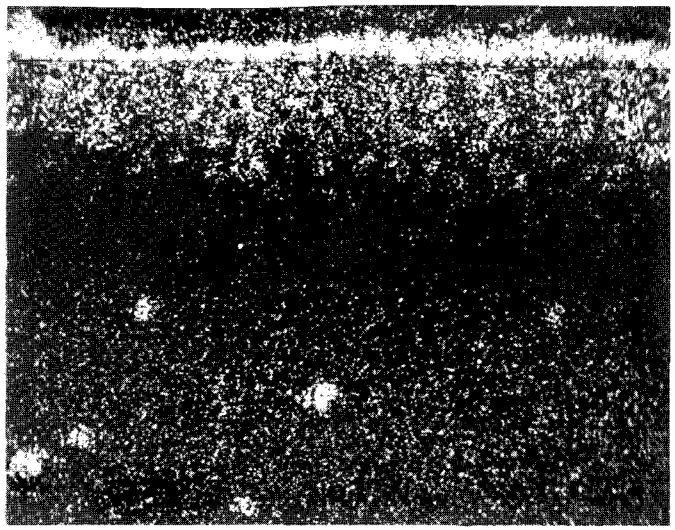

(g) Titanium.

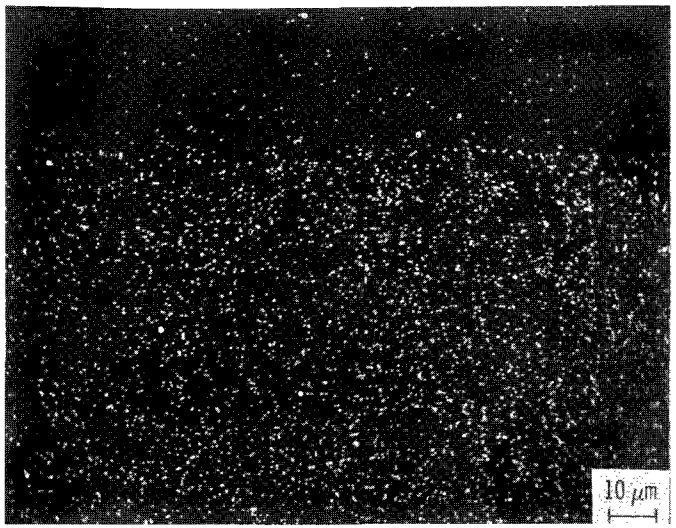

(h) Molybdenum.

Figure 14. - Concluded.

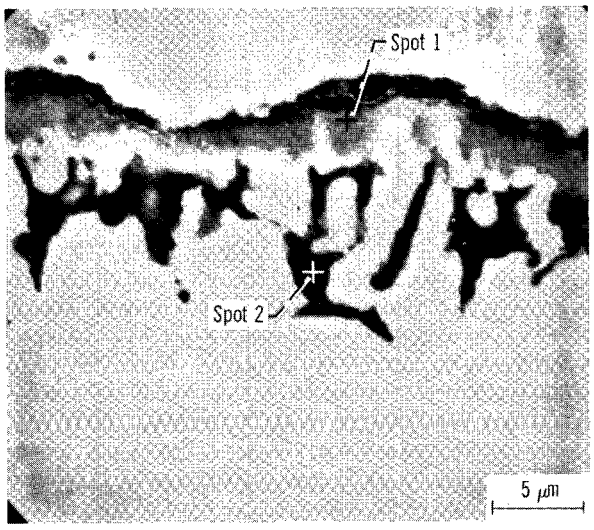

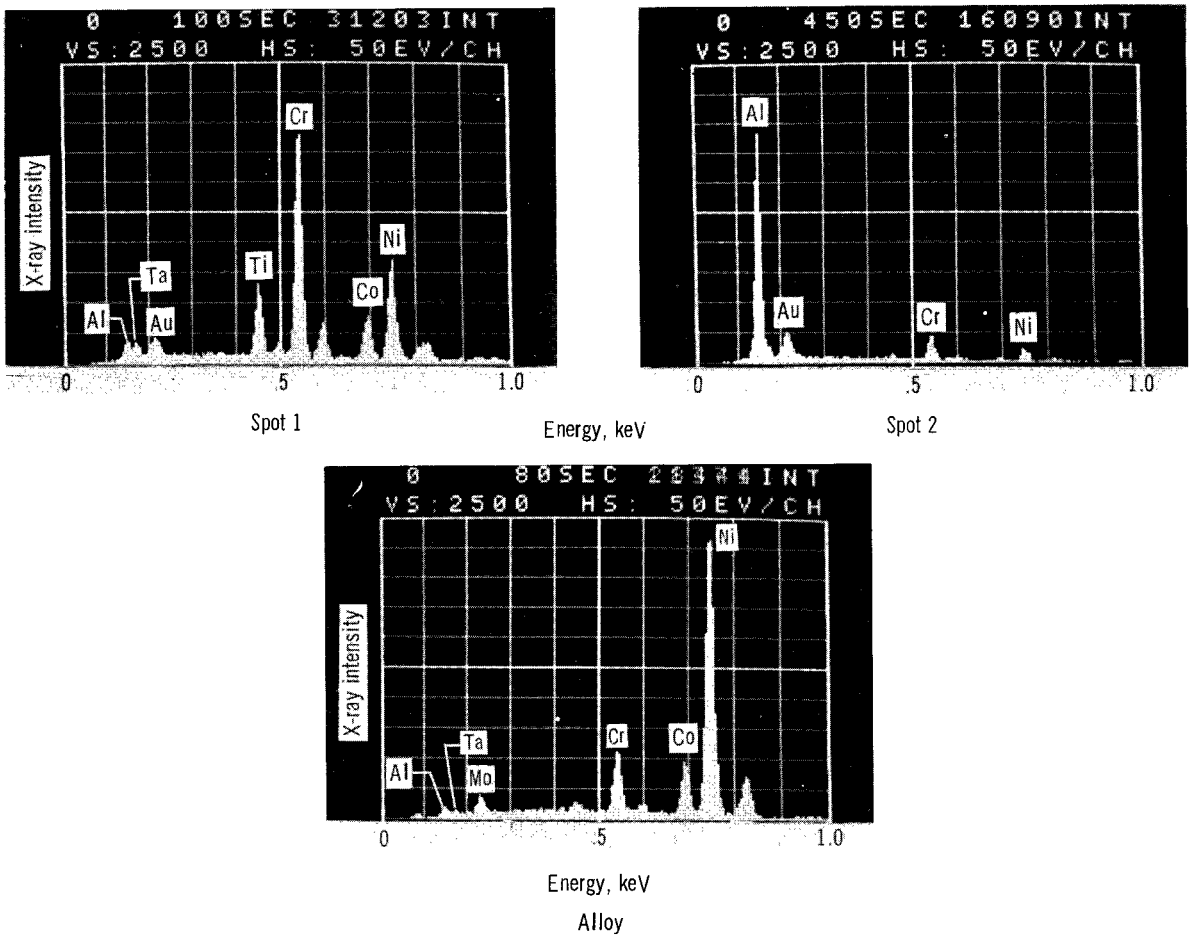

Figure 15. - SEM micrograph and EDS spectra of cross section of oxide scale formed on B-1900 at 900° C after 100 hours in slowly flowing oxygen.

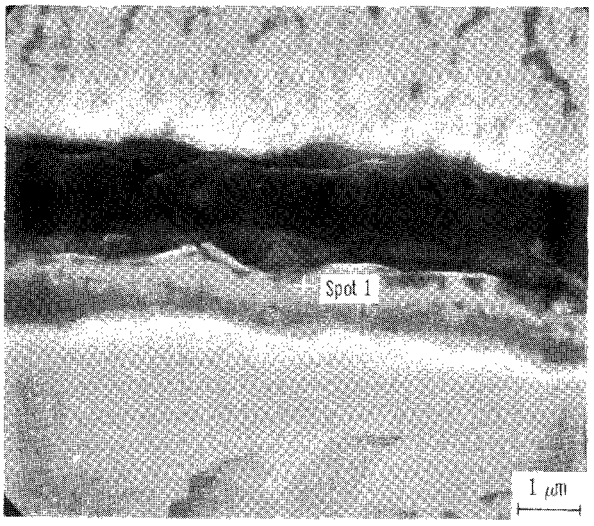

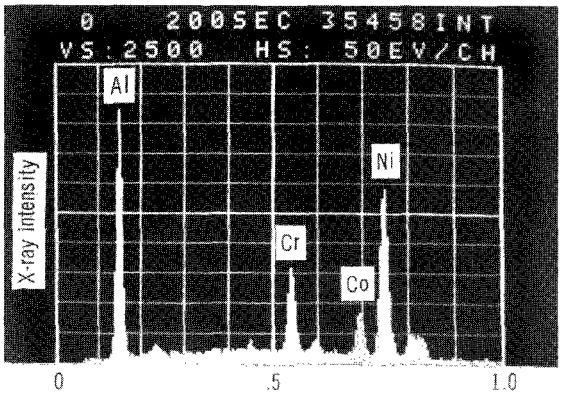

Energy, keV

Spot 1

Figure 16. - SEM micrograph and EDS spectra of cross section of oxide scale formed on B-1900 at 1000° C after 100 hours in slowly flowing oxygen.

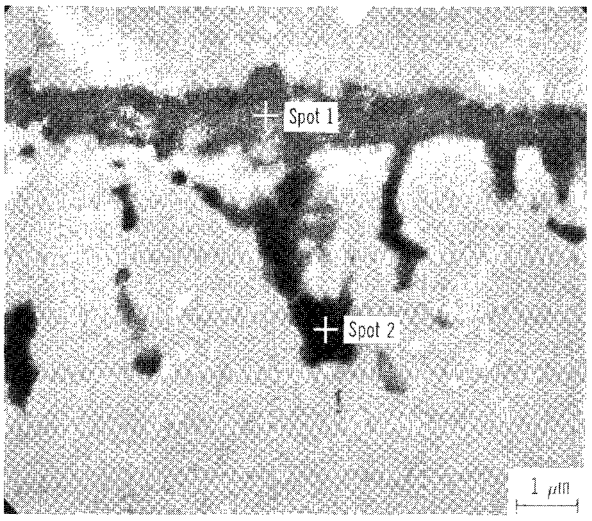

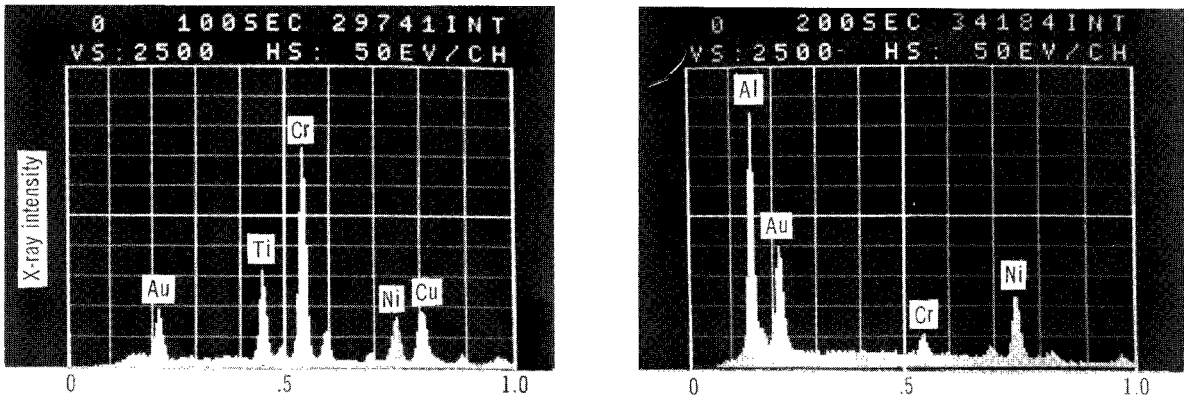

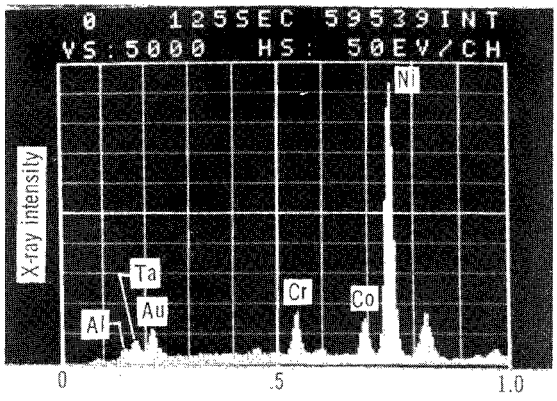

Figure 17. - SEM micrograph and EDS spectra of cross section of oxide scale formed on NASA-TRW VIA at 900° C after 100 hours in slowly flowing oxygen.

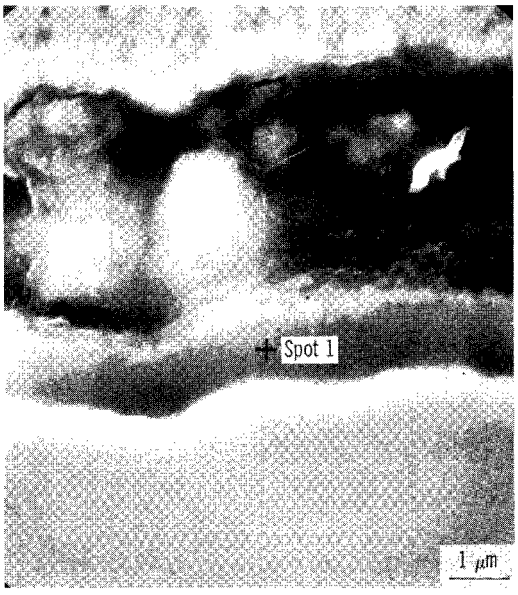

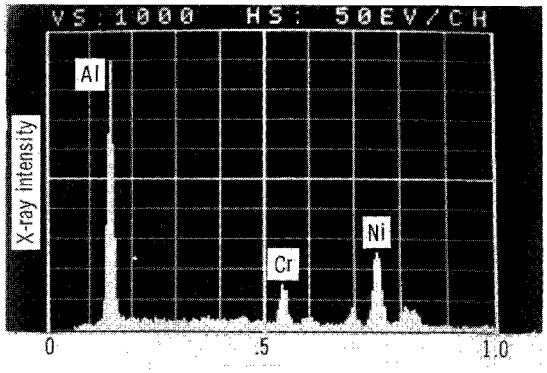

Spot 1

Figure 18. - SEM micrograph and EDS spectra of cross section of oxide scale formed on NASA-TRW VIA at 1000° C after 100 hours in slowly flowing oxygen.

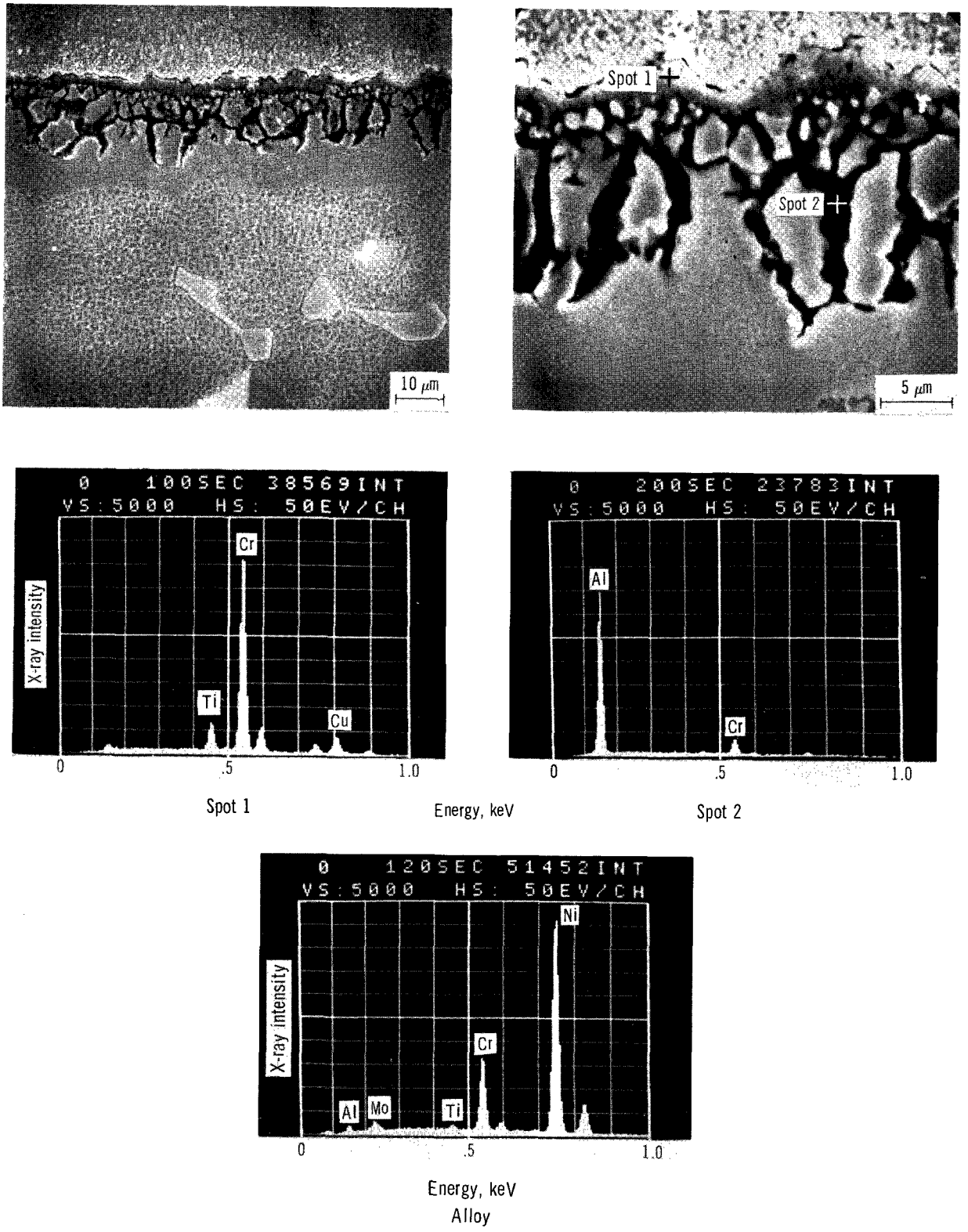

Figure 19. - SEM micrograph and EDS spectra of cross section of oxide scale formed on alloy 713C at 900° C after 100 hours in slowly flowing oxygen.

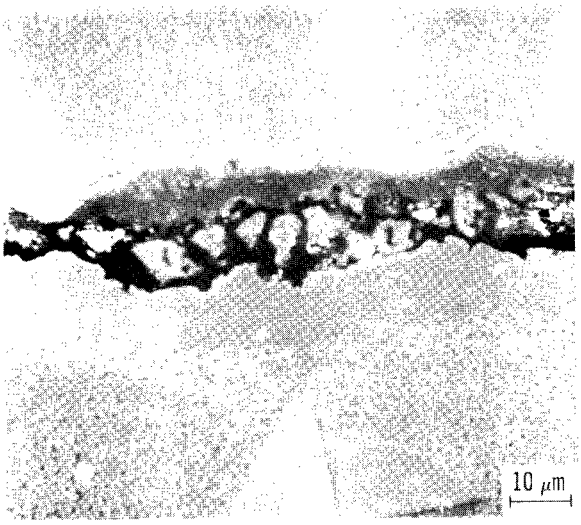

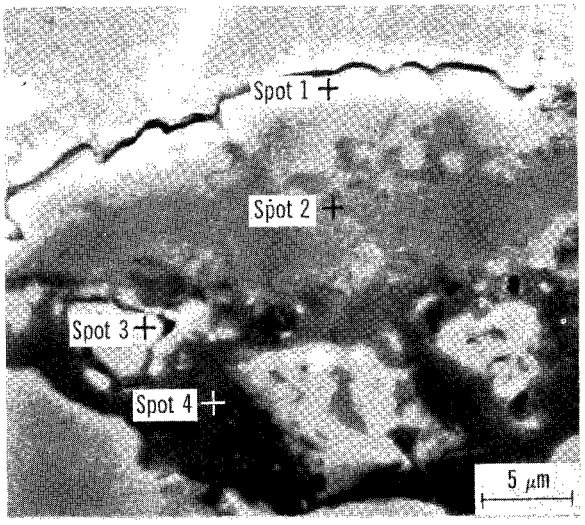

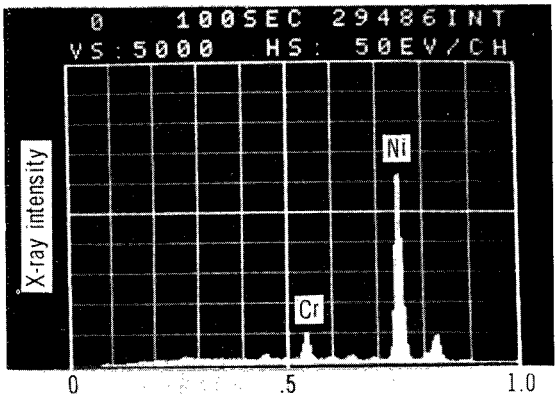

Spot 1

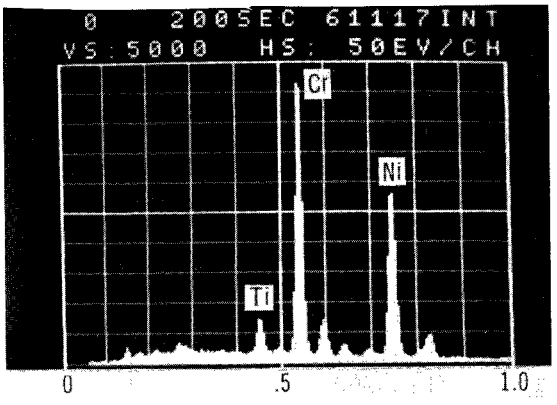

Spot 2

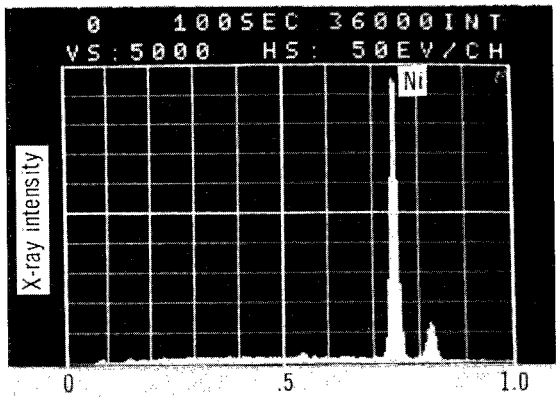

Spot 3

Energy, keV

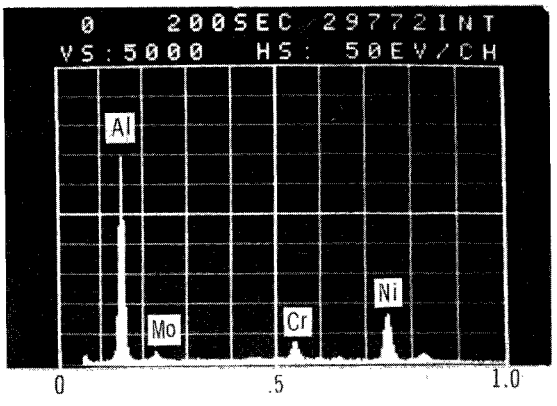

Spot 4

Figure 20. - SEM micrographs and EDS spectra of cross section of oxide scale formed on alloy 713C at 1000° C after 100 hours in slowly flowing oxygen.

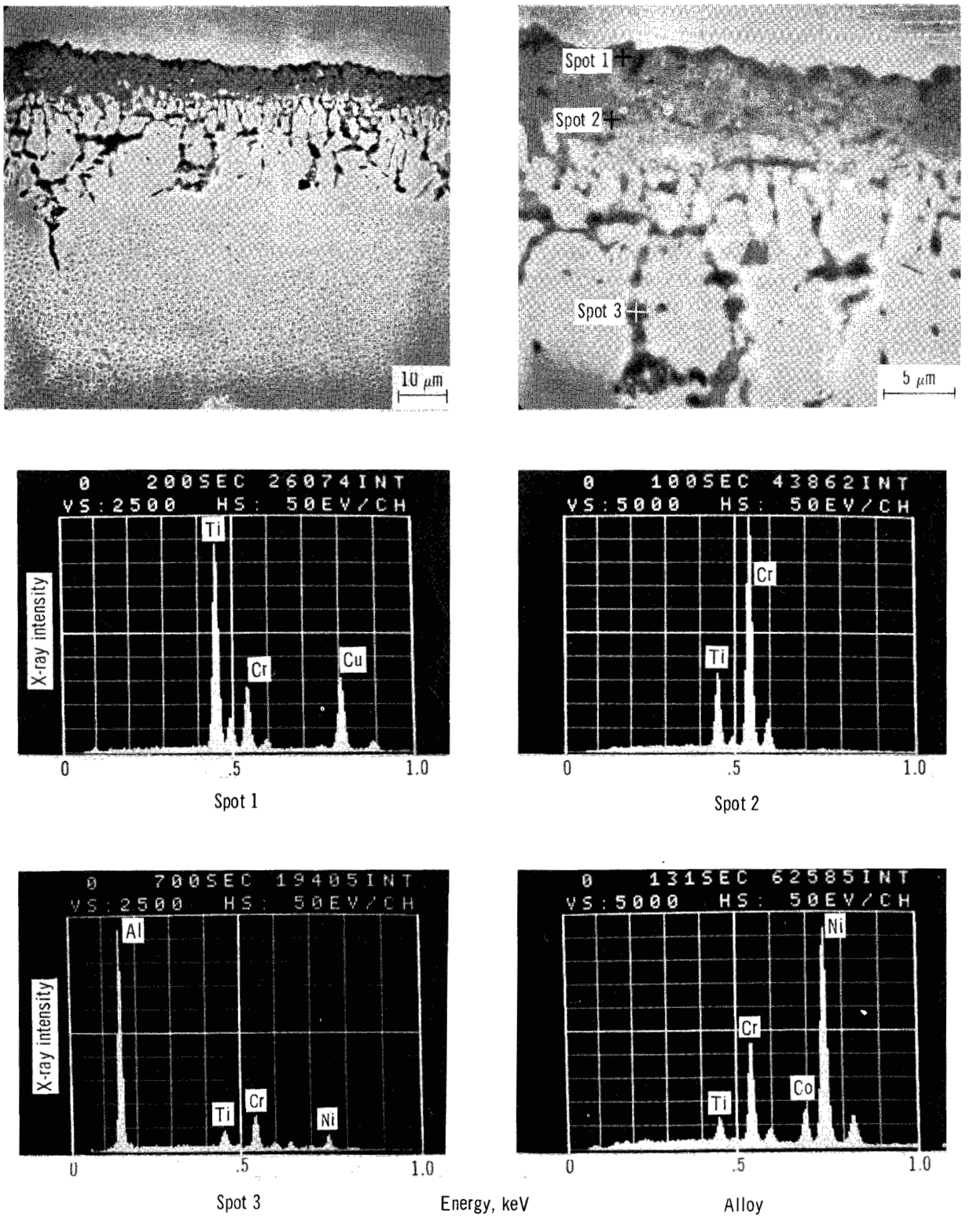

Figure 21. - SEM micrographs and EDS spectra of cross section of oxide scale formed on IN-738 at 900° C after 100 hours in slowly flowing oxygen.

NATIONAL AERONAUTICS AND SPACE ADMINISTRATION
WASHINGTON, D.C. 20546

OFFICIAL BUSINESS
PENALTY FOR PRIVATE USE $300

SPECIAL FOURTH-CLASS RATE
BOOK

POSTAGE AND FEES PAID
NATIONAL AERONAUTICS AND
SPACE ADMINISTRATION
451

U.S.MAIL

POSTMASTER: If Undeliverable (Section 158 Postal Manual) Do Not Return

"The aeronautical and space activities of the United States shall be conducted so as to contribute . . . to the expansion of human knowledge of phenomena in the atmosphere and space. The Administration shall provide for the widest practicable and appropriate dissemination of information concerning its activities and the results thereof."

—NATIONAL AERONAUTICS AND SPACE ACT OF 1958

NASA SCIENTIFIC AND TECHNICAL PUBLICATIONS

TECHNICAL REPORTS: Scientific and technical information considered important, complete, and a lasting contribution to existing knowledge.

TECHNICAL NOTES: Information less broad in scope but nevertheless of importance as a contribution to existing knowledge.

TECHNICAL MEMORANDUMS: Information receiving limited distribution because of preliminary data, security classification, or other reasons. Also includes conference proceedings with either limited or unlimited distribution.

CONTRACTOR REPORTS: Scientific and technical information generated under a NASA contract or grant and considered an important contribution to existing knowledge.

TECHNICAL TRANSLATIONS: Information published in a foreign language considered to merit NASA distribution in English.

SPECIAL PUBLICATIONS: Information derived from or of value to NASA activities. Publications include final reports of major projects, monographs, data compilations, handbooks, sourcebooks, and special bibliographies.

TECHNOLOGY UTILIZATION PUBLICATIONS: Information on technology used by NASA that may be of particular interest in commercial and other non-aerospace applications. Publications include Tech Briefs, Technology Utilization Reports and Technology Surveys.

Details on the availability of these publications may be obtained from:

SCIENTIFIC AND TECHNICAL INFORMATION OFFICE

NATIONAL AERONAUTICS AND SPACE ADMINISTRATION

Washington, D.C. 20546